with control mice.[13] Another study reported that a high-fat meal did not elicit changes in serum adiponectin compared with fasting baseline levels in healthy male subjects.[14] Thus, the effects of dietary fat intake on plasma adiponectin concentrations are unclear at present.

It is well established that atherosclerosis is a progressive multifactorial process that begins in early life.[15–17] However, few studies have examined the risk factors of atherosclerosis development in young women. In particular, the interaction between genes and environmental factors in the development of early atherosclerosis in young female populations is not clear. Thus, this study was designed to investigate the association between *AT1R* A1166C and plasma adiponectin concentrations in young female subjects. We also investigated the influence of *AT1R* A1166C on the correlation between dietary fat intake and plasma adiponectin concentrations in these subjects.

## METHODS

### Participants

Between July 2004 and December 2007, 416 students from 18 to 23 years of age were recruited from Mukogawa Women's University. We received approval from the Institutional Review Board and written informed consent was obtained from all participants in this study.

### Body composition and biochemical measurements

Blood samples were taken from each of the participants in the morning following overnight fasting. We measured the fasting plasma glucose, insulin, hemoglobin A1c (HbA1c), lipoprotein lipase (LPL), high-sensitivity C-reactive protein (hs-CRP), free fatty acid (FFA) and serum lipid concentrations including triglycerides (TG), high-density lipoprotein (HDL) cholesterol and low-density lipoprotein (LDL) cholesterol by standard laboratory techniques. Plasma levels of adiponectin and plasminogen-activator inhibitor 1 (PAI-1) were measured with commercial kits. Body composition was determined by dual-energy X-ray absorptiometry. Blood pressure was measured between 0900 and 1200 h (noon), with participants resting in the sitting position. Intima-media thickness (IMT) in the carotid artery was measured with the participants in a supine position after a few minutes of rest. Indices of obesity and insulin resistance were derived from body mass index (BMI) and a homeostasis model assessment of insulin resistance (HOMA-IR), respectively.

### Estimation of habitual food intake

Percentages of protein, fat and carbohydrate in the diet were estimated by using the responses to a self-administered diet history questionnaire, developed for use in the evaluation of nutrient intake levels and health education among both healthy individuals and high-risk populations. The diet history questionnaire was designed to obtain information about dietary habits for the previous month with regard to total energy and 17 nutrients.[18]

### Determination of AT1R A1166C polymorphism genotypes

Genomic DNA was extracted from 200 µl of whole blood, following the blood spin protocol recommended by the manufacturer for use of the QIAamp DNA Blood Kit (Qiagen Inc., Valencia, CA, USA). *AT1R* A1166C polymorphism genotypes were determined by the TaqMan polymerase chain reaction method. The primers and probes for genotype determinations were as follows: forward primer 5′-CATTCCTCTGCAGCACTTCACT-3′, reverse primer 5′-CGGTTC AGTCCACATAATGCAT-3′, probe for A (1166) 5′-FAM-CAAATGAGCAT TAGCTACMGB-3′, probe for C (1166) 5′-VIC-CAAATGAGCCTTAGCTACT-MGB-3′. Each reaction included 1 µl of the DNA sample including 30 ng of genetic DNA, 0.3 µl of each primer, 0.1 µl of each probe, 5 µl of the TaqMan Universal Master Mix (Applied Biosystems, Foster City, CA, USA) and 3.2 µl of sterile distilled water. Polymerase chain reaction cycling conditions were 1 cycle at 95 °C for 10 min, 45 cycles at 92 °C for 15 s and 60 °C for 1 min. Polymerase chain reaction and allelic detection were carried out using an ABI Sequence Detection System 7500 and allelic discrimination software, both from Applied Biosystems.

### Ultrasound studies

IMT was measured by ultrasonic diagnosis equipment (Shimazu SDU-2200, Shimazu, Tokyo, Japan) that was programmed with IMT software (Intima-scope, Media Cross Co. Ltd., Tokyo, Japan) as described.[19] This software makes it possible to automatically recognize the edges of the internal and the external membranes of the blood vessels and to automatically measure the distance at a sub-pixel level (estimated to be 0.01 mm), using a three-dimensional polynomial measurement formula.

Carotid artery ultrasonography was performed using a 10-MHz scanning frequency in B mode. One skilled observer, blinded to the subjective data, scanned the vessel in transverse planes. Subjects were examined in a supine position. Images were obtained in the 20 mm proximal to the origin of the bulb at the far wall of the right common carotid artery. In all subjects examined in this study, no plaque was observed in this segment. Average IMT was the average value of 250 computer-based points in the region.

### Statistical analysis

Agreement with the Hardy–Weinberg equilibrium was tested by comparing the observed and expected genotype frequencies of the participants using the $\chi^2$-test for good fit with Fisher's exact tests. On account of the very low frequency of the 1166C allele, participants who were homozygous for CC were combined in the analysis with those who were heterozygous AC to increase the statistical power. Normality of variable distribution was tested by the Kolmogorov–Smirnov test.

Quantitative data with a normal distribution were presented as the mean ± s.d., and data with a skewed distribution were presented as the median (interquartile range). Comparisons between carriers of the C allele and non-carriers were made using unpaired *t*-tests for continuous variables with normal distribution and with the nonparametric Mann–Whitney *U*-test for continuous variables with a skewed distribution. Pearson's and Spearman's coefficients of correlation were used as appropriate. A univariate generalized linear model was used to test for the heterogeneity of regression. To examine the independent contribution of the *AT1R* A1166C polymorphism to plasma adiponectin levels when adjusting for the effects of other clinical characteristics, logistic regression analysis with forward stepwise selection was used. For this analysis, participants were divided into two groups at the median of plasma adiponectin concentrations. We adjusted for confounders with the use of analysis of covariance (ANCOVA). To normalize variables with skewed distributions, logarithm, square root and inverse were used for data transformations as appropriate. Data were analyzed with SPSS (release 16.0J; SPSS Japan, Tokyo, Japan) and differences were considered significant with a *P*-value of $\leqslant 0.05$.

## RESULTS

### Genotype and participant characteristics

We examined the influence of *AT1R* A1166C on anthropometric features. The distributions of *AT1R* A1166C genotypes were as follows: *AT1R* A1166C AA, 83.2% ($n$=346); AC, 15.9% ($n$=66); and CC, 0.9% ($n$=4). The observed genotype frequencies in this study were in the Hardy–Weinberg equilibrium ($\chi^2$=0.185, $P$=0.912) and were similar to results from previous studies of Japanese populations.[20] There were no significant differences between carriers of the C allele and non-carriers in terms of age, height, weight, BMI, SBP, DBP, pulse rate, trunk fat mass, plasma concentrations of lipoproteins, plasma fasting glucose levels, HOMA-IR, HbA1c or IMT (Table 1). However, plasma adiponectin concentrations were significantly lower in carriers of the C allele compared with non-carriers. For comparison of plasma adiponectin concentrations between genotype groups, we used ANCOVA with BMI, HDL-Ch and HOMA-IR as covariates. The results of the evaluation of the assumptions of normality for sampling distributions and the homogeneity of variance were satisfactory. After adjustment by covariates, plasma adiponectin levels were significantly lower in carriers of the C allele compared with non-carriers ($P$=0.043) (Table 2). As shown in Table 3, multiple logistic regression analysis with forward stepwise selection, after controlling for age, BMI,

**Table 1 Characteristics and plasma adipocytokine concentrations of carriers and non-carriers of the C allele of the *AT1R* A1166C polymorphism**

| | n | *AA* | n | *AC+CC* | *P-value* |
|---|---|---|---|---|---|
| Age (years) | 346 | 20.0 (20.0–21.0) | 70 | 20.0 (19.0–21.0) | 0.050 |
| Height (cm) | 346 | 160.4 (157.0–164.2) | 70 | 162.4 (158.3–166.0) | 0.053 |
| Weight (kg) | 346 | 53.2 (49.3–58.8) | 70 | 54.7 (50.3–60.4) | 0.215 |
| BMI ($kg\,m^{-2}$) | 346 | 20.6 (19.4–22.1) | 70 | 20.6 (19.4–22.0) | 0.878 |
| TG ($mg\,dl^{-1}$) | 346 | 52.0 (41.0–68.3) | 70 | 45.5 (38.8–67.3) | 0.149 |
| HDL-Ch ($mg\,dl^{-1}$) | 346 | 74.0 (67.0–84.0) | 70 | 74.0 (63.8–82.3) | 0.474 |
| LDL-Ch ($mg\,dl^{-1}$) | 346 | 93.4 (78.8–109.7) | 70 | 90.2 (77.0–105.9) | 0.242 |
| Glucose ($mg\,dl^{-1}$) | 346 | 83.0 (79.0–88.0) | 70 | 83.0 (80.8–89.0) | 0.440 |
| HbA1c (%) | 346 | 4.8 (4.6–5.0) | 70 | 4.7 (4.6–4.9) | 0.145 |
| HOMA-IR | 342 | 1.1 (0.7–1.5) | 69 | 1.0 (0.7–1.6) | 0.792 |
| LPL ($ng\,dl^{-1}$) | 220 | 72.2 (60.2–85.3) | 40 | 79.5 (65.0–96.8) | 0.088 |
| SBP (mm Hg) | 346 | 106.5 (100.0–112.6) | 70 | 106.0 (99.0–113.1) | 0.699 |
| DBP (mm Hg) | 346 | 60.0 (55.5–66.1) | 70 | 60.3 (56.0–66.8) | 0.892 |
| Pulse rate (beats/min) | 344 | 60.0 (55.0–66.0) | 70 | 60.5 (53.0–69.0) | 0.781 |
| Trunk fat mass (kg) | 343 | 6.5 (5.3–8.1) | 69 | 6.6 (5.2–7.7) | 0.791 |
| IMT (mm) | 122 | 0.41 (0.37–0.45) | 18 | 0.44 (0.40–0.47) | 0.054 |
| Adiponectin ($\mu g\,ml^{-1}$) | 346 | 11.1 (8.4–14.2) | 70 | 10.2 (7.6–13.2) | 0.021* |
| PAI-1 ($ng\,ml^{-1}$) | 345 | 19.0 (13.0–26.0) | 69 | 19.0 (13.0–25.5) | 0.785 |

Abbreviations: BMI, body mass index; DBP, diastolic blood pressure; HDL, high-density lipoprotein, HOMA, homeostasis model assessment; IMT, Intima-media thickness; LDL, low-density lipoprotein; PAI-1, plasminogen-activator inhibitor 1; SBP, systolic blood pressure. Values are expressed as median (interquartile range). *$P<0.05$.

**Table 2 Analysis of covariance of genotype groups of *AT1R* A1166C toward plasma adiponectin concentration, with BMI, HDL-Ch and HOMA-IR as the covariates**

| *Source of variance* | *Adjusted sum of square* | *d.f.* | F | B | P-*value* |
|---|---|---|---|---|---|
| BMI | 3.184 | 1 | 8.567 | 17.187 | 0.004** |
| HDL-Ch | 13.164 | 1 | 35.459 | 0.229 | <0.001** |
| HOMAIR | 0.088 | 1 | 0.264 | −0.061 | 0.608 |
| Genotype | 1.531 | 1 | 4.123 | −0.164 | 0.043* |

Abbreviations: BMI, body mass index; HDL, high-density lipoprotein; HOMA, homeostasis model assessment.
Data transformation: BMI; Inverse, HDL-Ch; Square root, HOMA-IR; Logarithm. d.f.: degree of freedom, F:F value, *B*: standardized partial regression coefficient. *$P<0.05$, **$P<0.01$. Values are expressed as median (interquartile range).

**Table 3 Stepwise logistic regression analysis with above and below the median of plasma adiponectin concentrations as the dependent variable and selected variables as the independent variable**

| | | | | | *95% Confidence interval for odds ratio* | |
|---|---|---|---|---|---|---|
| *Variables* | B | *s.e.* | P-*value* | *Odds ratio* | *Lower* | *Upper* |
| C allele | 0.720 | 0.291 | 0.010 | 2.055 | 1.184 | 3.565 |
| BMI | 0.104 | 0.045 | 0.022 | 1.110 | 1.015 | 1.213 |
| HDL-Ch | −0.036 | 0.008 | <0.001 | 0.965 | 0.950 | 0.980 |

Abbreviations: BMI, body mass index; HDL, high density lipoprotein; TG, triglycerides.
B: partial regression coefficient. Not accepted variables were age, TG, HOMA-IR.

HDL-Ch, triglycerides and HOMA-IR, showed that the genotype with the C allele of the *AT1R* A1166C polymorphism was the strongest and the most independent determinant of lower plasma adiponectin concentrations (odds ratio: 2.055, 95% CI: 1.184–3.565, $P=0.010$), followed by BMI (odds ratio: 1.110, 95% CI: 1.015–1.213, $P=0.022$) and HDL-Ch (odds ratio: 0.965, 95% CI: 0.950–0.980, $P<0.001$). There were no significant differences, however, in plasma PAI-1 concentrations between these two groups.

Next, we examined whether clinical parameters differed between the participants in the lowest quartile of plasma adiponectin concentrations and those in the highest quartile. The participants in the lowest quartile of plasma adiponectin concentration showed significantly lower HDL-Ch and LPL levels and higher BMI and trunk fat mass when compared with participants in the highest quartile. Importantly, carotid IMT levels were significantly higher in the lowest quartile of plasma adiponectin concentrations than those in the highest quartile. No significant differences in low-density lipoprotein cholesterol, triglycerides, HOMA-IR and blood pressure, however, were observed between these groups (Table 4).

### Correlations between percentage of fat in the diet and plasma adiponectin concentrations in the genotype groups

Next, we examined the effects of dietary fat intake on plasma adiponectin concentrations in both genotypes. There were no significant differences in the mean or median intake of protein, fat and carbohydrate in the diet between carriers of the C allele and non-carriers (Table 5). Unexpectedly, a weak but significant positive correlation was found between the estimated percentages of fat in the diet and plasma adiponectin concentrations in non-carriers of the C allele ($r=0.161$, $P=0.004$) but not in carriers ($r=0.148$, $P=0.263$). There was no significant difference between the slopes of regression for carriers and non-carriers of the C allele ($P=0.731$) (Figure 1).

## DISCUSSION

In this study, we found that plasma adiponectin concentrations were significantly lower in carriers of the C allele of the *AT1R* A1166C gene polymorphism compared with non-carriers among a population of young Japanese women. To our knowledge, this report is the first to

**Table 4 Characteristics of the participants in the lowest or highest quartiles of plasma adiponectin concentrations**

| | *Plasma adiponectin concentrations* | | | | |
|---|---|---|---|---|---|
| | n | *The lowest quartile <8.3* | n | *The highest quartile 13.9≤* | P-*value* |
| BMI ($kg\,m^{-2}$) | 104 | 21.0 (19.7–22.4) | 105 | 20.4 (19.2–22.0) | 0.016* |
| Trunk fat mass (kg) | 104 | 7.1 (5.7–9.4) | 104 | 6.5 (5.3–7.4) | 0.003** |
| HDL-ch ($mg\,dl^{-1}$) | 104 | 69.0 (61.0–78.0) | 105 | 78.0 (68.0–90.0) | <0.001** |
| LDL-ch ($mg\,dl^{-1}$) | 104 | 93.5 ± 22.4 | 105 | 93.0 ± 23.1 | 0.869 |
| TG ($mg\,dl^{-1}$) | 104 | 60.5 (42.0–75.5) | 105 | 52.0 (38.5–65.5) | 0.060 |
| LPL ($ng\,ml^{-1}$) | 58 | 63.9 (55.1–76.1) | 79 | 79.4 (69.0–96.2) | <0.001** |
| HOMA-IR | 102 | 1.06 (0.74–1.67) | 104 | 1.09 (0.73–1.55) | 0.730 |
| Glucose ($mg\,dl^{-1}$) | 104 | 83.7 ± 6.5 | 105 | 83.3 ± 7.8 | 0.747 |
| HbA1c (%) | 104 | 4.8 (4.6–5.0) | 105 | 4.7 (4.6–4.9) | 0.390 |
| Leptin ($ng\,ml^{-1}$) | 104 | 8.1 (5.3–10.9) | 105 | 6.9 (5.2–9.5) | 0.049* |
| SBP (mm Hg) | 104 | 106.0 (99.6–114.8) | 105 | 108.0 (102.5–113.0) | 0.409 |
| DBP (mm Hg) | 104 | 61.8 (55.1–67.4) | 105 | 62.5 (57.0–68.0) | 0.260 |
| Pulse rate (beats/min) | 104 | 62.0 (55.3–67.8) | 105 | 58.0 (53.0–67.0) | 0.124 |
| IMT (mm) | 40 | 0.43 ± 0.06 | 45 | 0.39 ± 0.06 | 0.003** |

Abbreviations: BMI, body mass index; DBP, diastolic blood pressure; HbA1c, hemoglobin A1c; HDL, high-density lipoprotein, HOMA, homeostasis model assessment; IMT, Intima-media thickness; LDL, low-density lipoprotein; LPL, lipoprotein lipase; SBP, systolic blood pressure; TG, triglycerides.
Values are expressed as median (interquartile range) or mean ± s.d. *$P<0.05$, **$P<0.01$.

**Table 5 Estimated habitual food intakes in carriers and non-carriers of the C allele of the *AT1R* A1166C polymorphism**

| | n | *AA* | n | *AC+CC* | P-*value* |
|---|---|---|---|---|---|
| Fat (percentage of energy) | 309 | 30.1 (26.0–33.2) | 59 | 30.4 (27.0–33.6) | 0.852 |
| Carbohydrate (percentage of energy) | 309 | 54.8 (51.0–58.9) | 59 | 55.5 (50.7–58.9) | 0.996 |
| Protein (percentage of energy) | 309 | 13.3 ± 2.0 | 59 | 13.2 ± 2.3 | 0.803 |

Values are expressed as median (interquartile range) or mean ± s.d. *$P<0.05$.

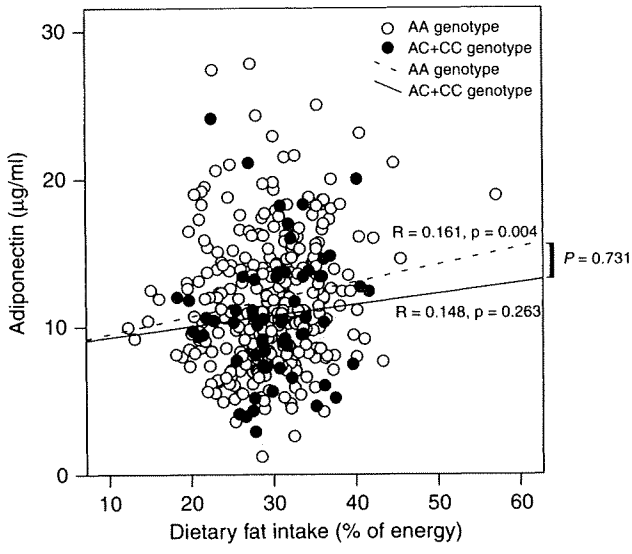


**Figure 1** Correlations between dietary fat intake (percentage of energy) and plasma concentrations of adiponectin.

show that the *AT1R* A1166C polymorphism may influence changes in plasma adiponectin concentrations in humans. Adiponectin is a unique and essential adipocytokine that is produced very abundantly from adipocytes and is stably present in the plasma at very high concentrations. Recent studies emphasize the part played by adiponectin in the homeostasis of adipose tissue and in the pathogenesis of the metabolic syndrome and atherosclerosis.[21] Adiponectin levels are positively correlated with HDL-cholesterol but inversely with insulin; the levels are reduced in obesity and type II diabetes[9] and lower in hypertensive patients compared with normotensive patients.[22] Plasma concentrations of adiponectin are, however, stable throughout the menstrual cycle[23] and also not affected by menopause in healthy women.[24]

Interestingly, participants in the lowest quartile of plasma adiponectin concentration had lower HDL-Ch and LPL levels and higher trunk fat mass compared with those in the highest quartile. In addition, the participants in the lowest quartile had thicker carotid IMT levels compared with those in the highest quartile. These results suggest that carriers of the C allele with lower adiponectin concentrations may be more susceptible to the development of atherosclerosis.

Although the mechanism underlying lower adiponectin concentrations in carriers of the C allele of the AT1R A1166C gene polymorphism is not clear at present, a silent polymorphism, A1166C, occurs in the 3′-untranslated region of the human *AT1R* gene that can lead to increased AT1R densities.[7] This suggests that the effect of AII may be enhanced in carriers of the C allele of the *AT1R* A1166C polymorphism.[4,25–27] It is noted that AII infusion decreases plasma adiponectin levels through its type 1 receptor in rats,[10] and treatment with an AII type 1 receptor antagonist increases plasma adiponectin levels in hypertensive patients.[12] These results suggest that a difference in activation of the local RAS may be directly involved in the variation between genotypes with regard to plasma adiponectin concentrations. However, further investigation is required to confirm this hypothesis.

In this study, we also found a genotype-dependent correlation between the percentage of fat in the diet and plasma adiponectin concentrations. Unexpectedly, there was a weak but significant positive correlation between plasma adiponectin concentrations and percentage of fat in the diet in non-carriers of the C allele, but not in carriers. Although the mechanism of this result is not clear, it was reported earlier that no correlation was found between dietary fat intake and plasma adiponectin concentration in humans,[14] suggesting that this relation may be specific for this genotype. Follow-up studies are necessary to clarify these points.

In conclusion, we showed that plasma adiponectin concentrations were associated with the C allele of the *AT1R* gene in young healthy women and that the *AT1R* genotype might affect plasma levels of adiponectin when these young women consume a high-fat diet. These results suggest that genotyping of the *AT1R* A1166C polymorphism may help to prevent the development of metabolic syndrome and atherosclerosis in young women.

## ACKNOWLEDGEMENTS

We thank Ms Sayaka Ohashi, Ms Kazuko Iwasa, Ms Seiko Kaji and Ms Eriko Nagata for laboratory and technical support during this investigation. This study was supported by a Grant-in-Aid for Scientific Research from the Japanese Ministry of Education, Science, Sports and Culture; also by the Open Research Center Project of Mukogawa Women's University for studying life-style-related diseases; by a Grant-in-Aid for Scientific Research (H17-pharmaco-common-003) from the Japanese Ministry of Health, Labor, and Welfare; Grants-in-Aid for Scientific Research (18590265, 18590811, 19650188) from the Ministry of Education, Science, Sports and Culture of Japan; and by research grants from the Takeda Science Foundation and the Japan Research Foundation for Clinical Pharmacology.

1 Prasad A, Quiyyumi AA. Renin-angiotensin system and angiotensin receptor blockers in the metabolic syndrome. *Circulation* 2004; **110**: 1507–1512.
2 Ogihara T, Asano T, Ando K, Chiba Y, Sakoda H, Anai M, Shojima N, Ono H, Onishi Y, Fujishiro M, Katagiri H, Fukushima Y, Kikuchi M, Noguchi N, Aburatani H, Komuro I, Fujita T. Angiotensin II—induced insulin resistance is associated with enhanced insulin signaling. *Hypertension* 2002; **40**: 872–879.
3 Engeli S, Negrel R, Sharma AM. Physiology and pathophysiology of the adipose tissue renin-angiotensin system. *Hypertension* 2000; **35**: 1270–1277.
4 Spiering W, Kroon AA, Fuss-Lejeune MMJJ, Daemen MJAP, de Leeuw PW. Angiotensin II sensitivity is associated with the angiotensin II type 1 receptor A1166C polymorphism in essential hypertensives on a high sodium diet. *Hypertension* 2000; **36**: 411–416.
5 Bonnardeaux A, Davies E, Jeunemaitre X, Charru A, Clause E, Tiret L, Cambien F, Corvol P, Soubrier F. Angiotensin II type 1 receptor gene polymorphisms in human essential hypertension. *Hypertension* 1994; **24**: 63–69.
6 Abdlooahi MR, Gaunt TR, Syddall HE, Cooper C, Phillips DIW, Ye S, Day INM. Angiotensin II type I receptor gene polymorphism: anthropometric and metabolic syndrome traits. *J Med Genet* 2005; **42**: 396–401.
7 Martin MM, Buckenberger JA, Jiang J, Malana GE, Nuovo GJ, Chotani M, Feldman DS, Schmittgen TD, Elton TS. The human angiotensin II type 1 receptor +1166 A/C polymorphism attenuates microRNA-155 binding. *J Biol Chem* 2007; **282**: 24262–24269.
8 Jaleel F, Jaleel A, Aftab J, Rahman MA. Relationship between adiponectin, glycemic control and blood lipids in diabetic type 2 postmenopausal women with and without complication of ischemic heart disease. *Clin Chim Acta* 2006; **370**: 76–81.
9 Mahmud A, Feely J. Adiponectin and arterial stiffness. *Am J Hypertens* 2005; **18**: 1543–1548.
10 Ran J, Hirano T, Fukui T, Saito K, Kageyama H, Okada K, Adachi M. Angiotensin II infusion decreases plasma adiponectin level via its type 1 receptor in rats: an implication for hypertension-related insulin resistance. *Metabolism* 2006; **55**: 478–488.
11 Furuhashi M, Ura N, Takizawa H, Yoshida D, Moniwa N, Murakami H, Higashiura K, Shimamoto K. Blockade of the renin-angiotensin system decreases adipocyte size with improvement in insulin sensitivity. *J Hypertens* 2004; **22**: 1977–1982.
12 Furuhashi M, Ura N, Higashiura K, Murakami H, Tanaka M, Moniwa N, Yoshida D, Shimamoto K. Blockade of the renin-angiotensin system increases adiponectin concentrations in patients with essential hypertension. *Hypertension* 2003; **42**: 76–81.
13 Zhou Q, Du J, Hu Z, Walsh K, Wang XH. Evidence for adipose –muscle cross talk: opposing regulation of muscle proteolysis by adiponectin and fatty acids. *Endocrinology* 2007; **148**: 5696–5705.
14 Poppitt SD, Keogh GF, Lithander FE, Wang Y, Mulvey TB, Chan YK, McArdle BH, Cooper GJS. Postprandial response of adiponectin, interleukin-6, tumor necrosis factor-α, and C-reactive protein to a high-fat dietary load. *Nutrition* 2008; **24**: 322–329.
15 Zieske AW, Tracy RP, McMahan CA, Herderick EE, Homma S, Malcom GT, Mcgill HC, Strong JP. Elevated serum C-reactive protein levels and advanced atherosclerosis in youth. *Arterioscler Thromb Vac Biol* 2005; **25**: 1237–1243.
16 Raitakari OT, Juonala M, Kahonen M, Taottonen L, Laitinen T, Maki-Torkko N, Jarvisalo MJ, Uhari M, Jokinen E, Ronnemaa T, Akerblom HK, Viikari JS. Cardiovascular risk factors in childhood and carotid artery intima-media thickness in adulthood. *JAMA* 2003; **290**: 2277–2283.
17 Knoflach M, Kiechl S, Kind M, Said M, Sief R, Gisinger M, van der Zee R, Gaston H, Jarosch E, Willeit J, Wick G. Cardiovascular risk factors and atherosclerosis in young males: ARMY study. *Circulation* 2003; **108**: 1064–1069.
18 Sasaki S, Yanagibori R, Amano K. Validity of a self-administered diet history questionnaire for assessment of sodium and potassium –Comparison with single 24-h urinary excretion. *Jpn Circ J* 1998; **62**: 431–435.
19 Yanase T, Nasu S, Mukuta Y, Shimizu Y, Nishihara T, Okabe T, Nomura M, Inoguchi T, Nawata H. Evaluation of a new carotid intima-media thickness measurement by B-mode ultrasonography using an innovative measurement software, intimascope. *Am J Hypertens* 2006; **19**: 1206–1212.
20 Kikuya M, Sugimoto K, Katsuya T, Suzuki M, Sato T, Funahashi J, Katoh R, Kazama I, Michimata M, Araki T, Hozawa A, Tsuji I, Ogihara T, Yanagisawa T, Imai Y, Mtsubara M. A/C1166 gene polymorphism of the angiotensin II type 1 receptor (AT1) and ambulatory blood pressure: the Ohasama Study. *Hypertens Res* 2003; **26**: 141–145.
21 Matsuzawa Y, Funahashi T, Kihara S, Shimomura I. Adiponectin and metabolic syndrome. *Arterioscler Thromb Vasc Biol* 2004; **24**: 29–33.
22 Tsuda K. Adiponectin and membrane fluidity of erythrocytes in normotensive and hypertensive men. *Obesity* 2006; **14**: 1505–1510.
23 Asimakopoulos B, Milousis A, Gioka T, Kabouromiti G, Gianisslis G, Troussa A, Simopoulou M, Katergari S, Tripsianis G, Nikolettos N. Serum pattern of circulation adipokines throughout the physiological menstrual cycle. *Endocr. J* 2009; Feb: 18.
24 Muscelli E, Kozakova M, Flyvbjerg A, Kyriakopoulou K, Astiarraga BD, Glintborg D, Konrad T, Favuzzi A, Petrie J. The effect of menopause on carotid artery remodeling, insulin sensitivity, and plasma adiponectin in healthy women. *Am J Hypertens* 2009; **22**: 354–370.
25 Van Geel PP, Pinto YM, Voors AA, Buikema H, Oosterga M, Crijns HJGM, van Gilst WH. Angiotensin II type 1 receptor A1166C gene polymorphism is associated with an increased response to angiotensin II in human arteries. *Hypertension* 2000; **35**: 717–721.
26 Nishikino M, Matsunaga T, Yasuda K, Adachi T, Moritani T, Tsujimoto G, Tsuda K, Aoki N. Genetic variation in the renin-angiotensin system and autonomic nervous system function in young healthy Japanese subjects. *J Clin Endocrinol Metab* 2006; **91**: 4676–4681.
27 Lim HS, Cho JY, Oh DS, Chung JY, Hong KS, Bae KS, Yu KS, Lee KH, Jang IJ, Shin SG. Angiotensin II type 1 receptor 1166A/C polymorphism in association with blood pressure response to exogenous angiotensin II. *Eur J Clin Pharmacol* 2007; **63**: 17–26.

*Endocrine Journal* 2009, **56** (6), 773-782

# Relationships of Systemic Oxidative Stress to Body Fat Distribution, Adipokines and Inflammatory Markers in Healthy Middle-aged Women

BIN WU*, KEISUKE FUKUO*, **, KAZUHISA SUZUKI*, **, GEN YOSHINO*** AND TSUTOMU KAZUMI*, **

**Open Research Center for Studying of Lifestyle-Related Diseases, Mukogawa Women's University, Nishinomiya, Hyogo, Japan*
***Department of Food Sciences and Nutrition, School of Human Environmental Science, Mukogawa Women's University, Nishinomiya, Hyogo, Japan*
****Department of Diabetes and Endocrinology, Toho University Omori Medical Center, Omori-Ku, Tokyo, Japan*

**Abstract.** Obesity and systemic oxidative stress are closely related. However data concerning the relationships between oxidative stress and body fat mass distribution are sparse. Anthropometric and metabolic profile was evaluated in 148 clinically healthy middle-aged women to assess the correlations between oxidative stress, fat mass distribution, adipokines, and inflammatory markers. Systemic oxidative stress was assessed by urinary creatinine-indexed 8-epi-prostaglandin $F_{2\alpha}$ (8-epi-$PGF_{2\alpha}$). Body fat mass distribution was examined by dual-energy X-ray absorptiometry (DXA). Lipid profile, adipokines and inflammatory markers including leptin, adiponectin, high sensitive C-reactive protein (hsCRP), plasminogen activator inhibitor-1 (PAI-1), tumor necrosis factor-α (TNF-α) were determined. We found body mass index (BMI), waist circumference (WC), both central and peripheral DXA-derived regional fat mass (FM) accumulations were positively correlated with 8-epi-$PGF_{2\alpha}$. Leptin, hsCRP and PAI-1also positively associated with 8-epi-$PGF_{2\alpha}$. After adjustment for BMI and WC, lower-body FM, total FM and PAI-1 retained significant association with 8-epi-$PGF_{2\alpha}$. Mutliple linear regression analyses indicated lower-body FM and PAI-1 were the two important predicators of 8-epi-$PGF_{2\alpha}$. These results suggest that DXA-derived regional FM indices, especially low extremity adiposity, are more closely associated with systemic oxidative stress than indirect anthropometric indices. Positive associations between 8-epi-$PGF_{2\alpha}$ and PAI-1, hsCRP, leptin support the notion that oxidative-stress-induced dysregulation of inflammation and adipokines may mediate the obesity-related metabolic derangement.

*Key words*: Oxidative stress, Body fat distribution, Adipokines

(*Endocrine Journal* **56**: 773-782, 2009)

**OBESITY** is the principle causative factor and main component of metabolic syndrome (MetS) [1]. MetS is associated with high risk for the development of diabetes and cardiovascular diseases (CVD)[2]. However, the underlying mechanisms linking obesity with MetS have not been fully elucidated. It is well known that overproduction of some adipokines, including TNF-α [3] and PAI-1 [4] in adipose tissue may lead to the development of insulin resistance and atherosclerosis. But the factors regulating the production and secretion of such adipokines in adipose tissue have not been clearly understood.

Oxidative stress is one of the important pathways that involves in atherosclerosis [5, 6], endothelial dysfunction [7] and diabetes [8]. Recently it is reported that in cultured adipocytes, increased oxidative stress may cause deregulated production of adipokines, including leptin, adiponectin, PAI-1 and monocyte chemotactic protein-1 (MCP-1) thus lead to metabolic derangements [9]. Various cross-sectional studies implicated a significant positive relationship of systemic oxidative stress with obesity–related indices such as BMI and WC [9-12]. Obesity is regarded as a hyper-oxida-

Received Nov. 14, 2008; Accepted May 15, 2009 as K08E-332
Released online in J-STAGE as advance publication Jun. 9, 2009

Correspondence to: Bin WU, Open Research Center for Studying of Lifestyle-Related Diseases, Mukogawa Women's University 6-46, Ikebiraki-cho, Nishinomiya, Hyogo, 663-8558, Japan.
E-mail: wu.bin@gmx.com

tive and chronic inflammatory status, the significant interrelationships among obesity-related indices, oxidative stress, inflammatory markers and adipokines have been well documented [10, 11, 13-15]. However, most of the studies just examined the indirect anthropometric indices such as BMI and WC as well as their relationships with systemic oxidative stress [10, 11, 15], or focused on the association between certain regional adiposity (abdomen) and oxidative stress without taking total body FM and pattern of distribution into consideration [12, 16]. Because adipose tissue accumulating in different anatomic compartments (regional adiposity) may have unique characteristics related to different expression of enzymes and receptors involving in triglyceride synthesis [17], lipolysis [18] and adipokine synthesis [18], and lines of evidence also suggested that different regional adiposity have different clinical implications [19], for instance, abdominal (central) adiposity is closely related with high CVD risks [2] whereas lower-body (peripheral) adiposity is reported to relate with a favorable lipid profile against the adverse effects of obesity [19-22]. Therefore it is essential to exam the relationship between regional adiposity and oxidative stress, and to further identify the role of oxidative stress in mediating metabolic effects of regional adiposity. Until now regional adiposity and its correlation with systemic oxidative stress has not been well documented.

In the present study, cross-sectional study was conducted in a middle-aged clinically healthy female cohort. Systemic oxidative stress was evaluated by urinary creatinine-indexed 8-epi-prostaglandin $F_{-2\alpha}$ (8-epi-$PGF_{2\alpha}$), a validated biomarker of oxidative stress [23]. Body fat mass distribution was examined by dual-energy X-ray absorptiometry (DXA). Their relationships with obesity-related metabolic characteristics, including inflammatory markers, adipokines, and lipid profile were investigated. Men and women have different FM distribution pattern. FM tends to depot in the abdominal/central region in men whereas women tend to accumulate FM in the lower-body/peripheral region [24]. Substantial evidence has demonstrated that sex-differences in the FM distribution may lead to distinct metabolic outcomes [25], therefore this study we only included women as subjects in order to keep the confounding factors as low as possible.

## Materials and Methods

*Subjects*

148 middle-aged (39-60 years) clinically healthy women participated in this study. There were 137 (92.6%) pre-menopause and 11 (7.4%) post-menopause women. Subjects with clinical diagnosed endocrine, cardiovascular, hepatic, renal diseases, hormonal contraception or replacement, cigarette smokers and alcohol consuming ≥40g/day were excluded. Nobody received any medications or antioxidative vitamins. The study was approved by the Ethics Committees of Mukogawa Women's University and written informed consents were obtained from all participants.

*Anthropometry, body composition and fat mass distribution*

Body weight, height, WC were measured following standard procedures and BMI was calculated. DXA with a scanner (Hologic QDR-2000, software version 7.20D, Bedford, MA) was applied to measure body mass distribution. This method uses a three-compartments model of body mass and provides an estimate of regional fat mass (FM), lean tissue and bone mineral. A scanned image of the whole body was divided into six subdivisions: head, trunk, left and right arms and lower-body (Fig. 1). The dividing borders between those subregions were differentiated by a line underneath the chin, a line between the humerus head and the glenoid fossa, and a line at the femoral neck. The trunk region included the chest and abdomen, excluding the pelvis. The lower-body region included the entire hip, thigh, and leg [25]. Regional FM ratios (%FM) were expressed as percentage of regional fat tissue weight/regional body weight×100%. DXA is considered to be the gold standard for determination of body fat and pattern of distribution with lower radiation exposure and less time-consuming compared with computer tomography (CT) scan [26, 27] .

*Insulin, glucose, and insulin resistance*

Blood samples were obtained in the morning after 12-hr overnight fast. Insulin resistance determined by homeostasis model assessment (HOMA-IR) were calculated using fasting plasma glucose and insulin levels [28].

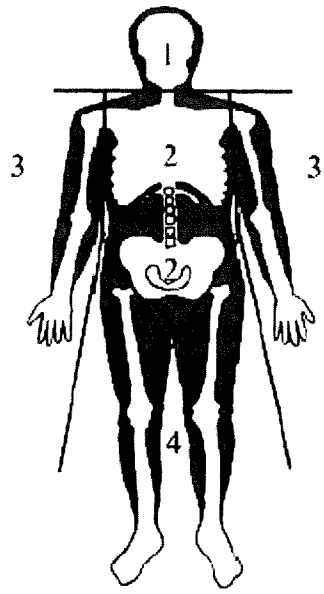


**Fig. 1.** Standard regions of a dual-energy X-ray absorptiometry scan 1, head; 2, trunk; 3, arms; 4, lower-body

*Plasma lipids, lipoprotein, and Apo measurements*

Serum lipids [triglycerides (TG), total cholesterol (TC), high-density lipoprotein cholesterol (HDL-C) ] were measured using an autoanalyzer (AU5232, Olympus, Tokyo, Japan). Apolipoprotein A-1 (ApoA1), and apolipoprotein B-100 (ApoB) were measured by respective commercially available kits using an Olympus autoanalyzer (AU600, Mitsubishi Chemicals, Tokyo, Japan). Low-density lipoprotein cholesterol (LDL-C) was determined using the Friedewald formula [29]. Small density LDL-C (sd LDL) was measured by a precipitation method described elsewhere [30].

*Oxidative stress, adipokines, and inflammatory markers*

Urinary 8-epi-$PGF_{2\alpha}$ was measured in the first-voided morning urine sample with an enzyme-liked immunosorbent assay (8-Isoprostane EIA kit, Cayman, Ann Arbor, MI). Intra- and inter- assay CV were 7.5% and 9.2%, respectively. Urinary 8-epi-$PGF_{2\alpha}$ was indexed to creatinine as picograms per milligram creatinine. Adiponectin was assayed by a sandwich enzyme-linked immunosorbent assay (Otsuka Pharmaceutical Co., Ltd., Tokushima City, Japan). Intra- and inter-assay CV were 3.3% and 7.5%, respectively. Leptin were assessed by a RIA kit from LINCO research (St. Charles, MO, interassay CV=4.9%). Highly sensitive C-reactive protein (hsCRP) was measured by an immunoturbidometric assay with the use of reagents and calibrators from Dade Behring Marbura GmbH (Marburg, Germany; interassay CV<5.0%). TNF-α were measured by immunoassays (R&D Systems, Inc., Minneapolis, MN, interassay CV = 6.0%). PAI-1 was measured by an ELISA method (Mitsubishi Chemicals, interassay CV= 8.1 %). For statistical analysis, serum concentrations of hsCRP and TNF-α below the limit of detection were assigned a value of 50μg/liter and 50pg/mL (the lowest limit of detection), respectively.

*Statistics*

Data were presented as mean±SD. Due to deviation from normal distribution, hsCRP was logarithmic transformed for analysis. Means differences among groups were compared by nonparametric Mann-Whitney U test or ANOVA with Bonferroni correction for multiple comparisons. Univariate correlations of urinary 8-epi-$PGF_{2\alpha}$ with regional FM distribution, and other metabolic parameters were evaluate with both Spearman's rank order and Pearson correlation coefficients. Both methods gave practical identical results, and only Spearman's coefficients were reported here. Stepwise multiple regression analyses were performed to further indentify the most significant variables contributing to the variation of 8-epi-$PGF_{2\alpha}$. All the variables with significant associations with 8-epi-$PGF_{2\alpha}$ in univariate analyses were entered into the model simultaneously. In each following step, the variable having the least significant $P$ value was excluded from the model. Finally, all variables with $P<0.05$ remained in the model. Standardized ß-estimate was used to determine which variable had the strongest effect on 8-epi-$PGF_{2\alpha}$. A two-tailed $P<0.05$ was considered statistically significant. All calculations were performed with SPSS system 15.0 (SPSS Inc, Chicago, IL).

## Results

According to the Asian-Pacific redefining criteria of obesity [31], there were 106 normal weight (BMI<23kg/$m^2$) and 42 over weight (BMI≥23kg/$m^2$) subjects and nobody could be classified as MetS according to NCEP ATP III [32], IDF [33], or Japanese

**Table 1.** Anthropometric and metabolic characteristics of the subjects

| | Normal weight (n=102) | Over weight (n=46) | *P* value |
|---|---|---|---|
| Age (year) | 49.7±3.6 | 50.0±3.7 | 0.914 |
| BMI (kg/m$^2$) | 20.4±1.5 | 25.4±2.0 | <0.001 |
| Waist circumeference (cm) | 75.1±5.7 | 86.6±6.9 | <0.001 |
| Total FM (kg) | 13.435±4.184 | 21.957±4.967 | <0.001 |
| %Total FM | 27.3±6.2 | 36.4±5.2 | <0.001 |
| Trunk FM (kg) | 7.066±2.502 | 12.276±2.855 | <0.001 |
| %Trunk FM | 29.4±7.5 | 40.4±5.7 | <0.001 |
| Arm FM(kg) | 1.189±0.536 | 2.117±0.64 | <0.001 |
| %Arm FM | 24.8±8.1 | 34.4±6.1 | <0.001 |
| Lower- Body FM (kg) | 4.606±1.361 | 6.809±1.881 | <0.001 |
| %Lower- Body FM | 28.2±5.9 | 34.9±6.1 | <0.001 |
| $HbA_{1C}$ (%) | 5.0±0.3 | 5.3±0.6 | <0.001 |
| HOMA-IR | 1.03±0.57 | 1.61±0.83 | <0.001 |
| Triglyceride (mmol/L) | 0.85±0.35 | 1.06±0.48 | 0.011 |
| Total Cholesterol (mmol/L) | 5.79±0.89 | 5.77±0.92 | 0.969 |
| HDL Cholesterol (mmol/L) | 2.09±0.38 | 1.80±0.41 | <0.001 |
| LDL Cholesterol (mmol/L) | 3.31±0.74 | 3.48±0.82 | 0.255 |
| sd LDL (mg/dL) | 15.15±8.23 | 22.55±10.11 | <0.001 |
| ApoA1 (mg/dL) | 182.0±21.3 | 168.6±21.5 | 0.001 |
| ApoB (mg/dL) | 89.7±18.3 | 99.3±20.0 | 0.003 |
| Leptin (ng/mL) | 5.9±3.1 | 11.3±6.0 | <0.001 |
| Adiponectin (μg/mL) | 12.6±5.2 | 10.1±3.9 | 0.004 |
| PAI-1 (ng/mL) | 19.5±11.2 | 33.7±17.7 | <0.001 |
| LogCRP | 1.28±0.49 | 1.71±0.49 | <0.001 |
| TNF-α (pg/mL) | 0.75±0.32 | 0.83±0.49 | 0.413 |
| sBP (mmHg) | 116.2±11.6 | 131.7±18.0 | <0.001 |
| dBP (mmHg) | 71.3±9.1 | 78.5±12.5 | 0.001 |
| 8-epi-$PGF_{2\alpha}$ (pg/mg.creatinine) | 338.6±133.7 | 430.4±258.3 | 0.008 |

Data are the means±SD.BMI, body mass index; FM, fat mss; HOMA-IR, homeostasis model assessment of insulin resistance; sBP, systolic blood pressure; dBP, diastolic blood pressure; sd LDL, small density LDL.

criteria [34]. Their anthropometric and metabolic characteristics were presented in Table 1. Over weight subjects showed higher both indirect anthropometric measurements (BMI, WC) and direct anthropometric measurements (DXA-indices), all the $P<0.001$. For lipid profile, TG, HDL-cholesterol, sd LDL, ApoA1 and ApoB were difference between two groups. HOMA-IR was significantly higher in over weight than normal weight ($P<0.001$). For adipokines and inflammatory markers, leptin, adiponectin, Log (hsCRP), PAI-1 were significantly different between two groups. Urinary 8-epi-$PGF_{2\alpha}$ excretion of over weight subjects was ~ 30% higher than that of normal weight women ($P=0.002$). We also used 25kg/m$^2$ as BMI cutoff point to divide total subjects into normal weight and over weight group, and the comparisons gave the approximatively identical results (data not shown).

In the univariate correlation analyses (Table 2), 8-epi-$PGF_{2\alpha}$ correlated with all anthropometric parameters, systolic BP and diastolic BP. Among them, the strongest correlations were found among 8-epi-$PGF_{2\alpha}$, lower-body FM, total FM and trunk FM (r=0.353, 0.295, and 0.263, all the $P<0.001$, Fig.2A, 2B, 2C). For metabolic parameters, 8-epi-$PGF_{2\alpha}$ had significant correlations with PAI-1 (r=0.237, $P<0.05$), [Log (hsCRP), r=0.164, $P<0.05$], leptin (r=0.175, $P<0.05$). According to the body FM content (%total FM), 148 women were stratified into high (≥30%, n=72) and

**Table 2.** Characteristics of all subjects and correlation coefficients with 8-epi-PGF2α

| Total subjetcs (n=148) | Mean±SD | r | *P* value |
|---|---|---|---|
| Age (year) | 49.8±3.6 | 0.056 | 0.499 |
| BMI (kg/m$^2$) | 22.0±2.8 | 0.238 | 0.004 |
| Waist circumeference (cm) | 78.7±8.1 | 0.230 | 0.009 |
| Total FM (kg) | 16.062±5.929 | 0.295 | <0.001 |
| %Total FM | 30.1±7.3 | 0.290 | <0.001 |
| Trunk FM (kg) | 8.672±3.552 | 0.263 | 0.001 |
| %Trunk FM | 32.9±8.7 | 0.246 | 0.003 |
| Arm FM (kg) | 1.475±0.712 | 0.250 | 0.002 |
| %Arm FM | 27.8±8.8 | 0.254 | 0.002 |
| Lower-Body FM (kg) | 5.285±1.842 | 0.353 | <0.001 |
| %Lower- Body FM | 30.3±6.7 | 0.342 | <0.001 |
| $HbA_{1c}$(%) | 5.1±0.4 | 0.100 | 0.225 |
| HOMA-IR | 1.21±0.71 | 0.088 | 0.288 |
| Triglyceride (mmol/L) | 0.92±0.4 | -0.029 | 0.725 |
| Total Cholesterol (mmol/L) | 5.78±0.9 | -0.122 | 0.138 |
| HDL Cholesterol (mmol/L) | 2.00±0.41 | -0.036 | 0.66 |
| LDL Cholesterol (mmol/L) | 3.37±0.77 | -0.146 | 0.077 |
| sd LDL (mg/dL) | 17.48±9.47 | -0.141 | 0.14 |
| ApoA1 (mg/dL) | 177.9±22.2 | -0.014 | 0.867 |
| ApoB (mg/dL) | 92.7±19.3 | -0.087 | 0.292 |
| Leptin (ng/mL) | 7.6±4.9 | 0.175 | 0.033 |
| Adiponectin (μg/mL) | 11.8±4.9 | 0.083 | 0.314 |
| PAI-1 (ng/mL) | 23.9±15 | 0.237 | 0.018 |
| LogCRP | 1.41±0.53 | 0.164 | 0.021 |
| TNF-α (pg/mL) | 0.77±0.38 | 0.047 | 0.569 |
| sBP (mmHg) | 120.0±15.6 | 0.199 | 0.015 |
| dBP (mmHg) | 73.5±10.8 | 0.149 | 0.041 |
| 8-epi-$PGF_{2\alpha}$ (pg/mg.creatinine) | 367.1±185.8 | | |

Data are the means±SD.BMI, body mass index; FM, fat mss; HOMA-IR, homeostasis model assessment of insulin resistance; sBP, systolic blood pressure; dBP, diastolic blood pressure; sd LDL, small density LDL.

normal (<30%, n=76) subgroups. Significant correlations between lower-body FM and urinary 8-epi-$PGF_{2\alpha}$ excretion were observed in both two groups (for high FM content group, r=0.224, *P*=0.048; for normal FM content group, r=0.315, *P*=0.007).

Because there were strong interrelationships between BMI, WC and DXA indices, all the univariate analyses were repeated after adjustment for BMI and WC. After this correction, the following parameters retained significant correlations with 8-epi-$PGF_{2\alpha}$: lower-body FM (partial r=0.262 *P*=0.004), total FM (partial r=0.218 *P*=0.018) and PAI-1 (partial r=0.208 *P*=0.024). Associations between 8-epi-$PGF_{2\alpha}$ and BMI, WC were disappeared after adjustment for DXA-derived total FM.

The stepwise regression analysis revealed that 11.2% variance of in 8-epi-$PGF_{2\alpha}$ in all study subjects was predicted by lower-body FM and PAI-1 (Table 3). Lower-body FM was the first variable accepted in the model, which account for 8.4% of the variance of 8-epi-$PGF_{2\alpha}$. PAI-1 was the second variable accepted in the model, which contribute 5.0% variance of 8-epi-$PGF_{2\alpha}$ independently.

We compared the urinary 8-epi-$PGF_{2\alpha}$ levels divided by tertile of trunk FM and WC, two surrogate indices for visceral fat accumulation. Among all subjects, 8-epi-$PGF_{2\alpha}$ were significantly increased across the low, middle and high categories of trunk FM

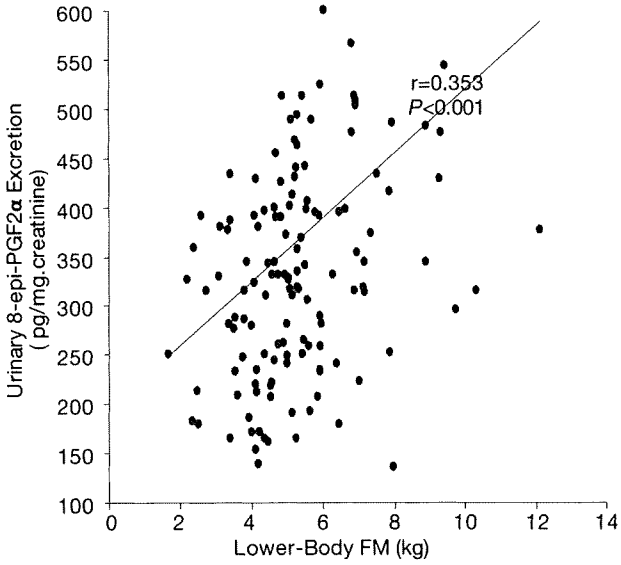


**Fig. 2A.** Relationship between lower-body fat mass (FM)and urinary 8-epi-$PGF_{2\alpha}$

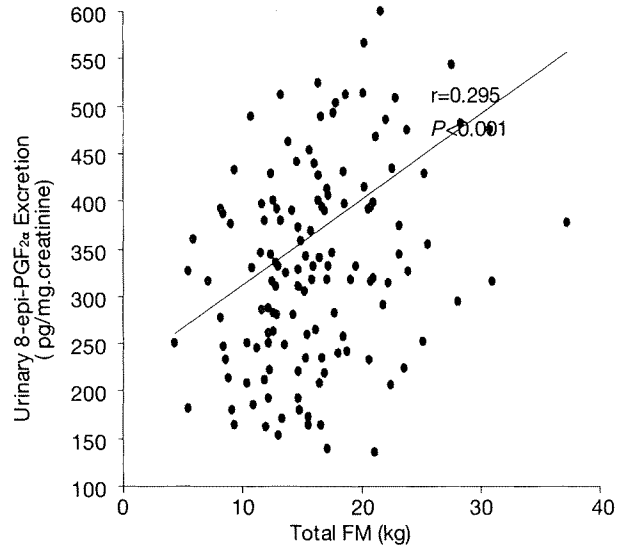


**Fig 2B** Relationship between total fat mass (FM) and urinary 8-epi-$PGF_{2\alpha}$

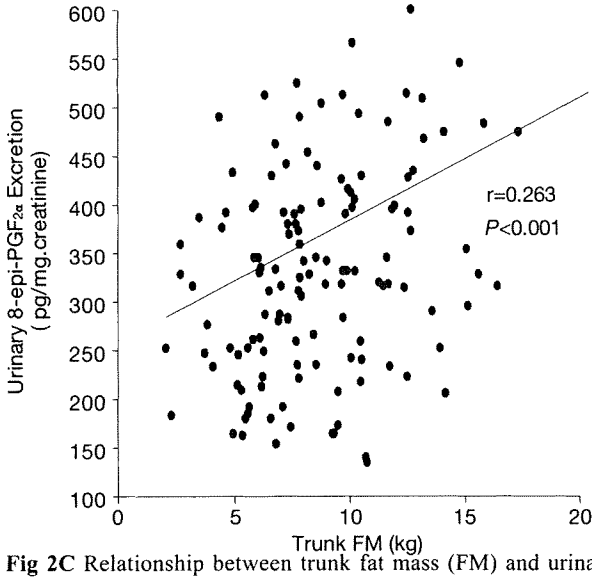


**Fig 2C** Relationship between trunk fat mass (FM) and urinary 8-epi-$PGF_{2\alpha}$

(for trunk FM category: 334.6±158.0, 346.8±115.3, 424.2±253.0, *P* for trend <0.01) and WC (for WC category: 334.6±135.8, 337.3±129.0, 428.1±252.0, *P* for trend <0.01). Finally, by using Japanese criteria [34] the subjects were divided into 3 groups according to their components of MetS: with 0 risk factor (n=81), 1 risk factor (n=37) and ≥2 risk factors (n=30). Urinary 8-epi-$PGF_{2\alpha}$ excretion were significantly higher in 2 or more risk factors group than 0 and 1 risk factor groups (460.0±204.1 *vs* 337.8±135.9, 355.9±127.1, *P*=0.002 and 0.020, respectively).

**Table 3.** Multiple regression analysis for estimation of 8-epi-PGF2α in 148 healthy middle-aged women.

| Independent variables | standard β coefficients | Adjusted $R^2$ | *P* value |
|---|---|---|---|
| constant | 174 | | <0.001 |
| lower-body FM | 0.258 | 0.084 | 0.002 |
| PAI-1 | 0.190 | 0.112 | 0.019 |

n=148, This model includes all the variables which have significant association with 8-epi-$PGF_{2\alpha}$ in Table 2.

## Discussion

Oxidative stress is recognized to be a prominent feature of CVD [5, 6] and MetS [16, 35]. The measurement of F2-isoprostane is the most reliable approach to estimate oxidative stress status and lipid peroxidation *in vivo* [26]. In the present study, we demonstrated that all the DXA-derived fat mass indices have positive relationships with systemic oxidative stress in healthy middle-aged women. Furthermore, the observations that subjects with higher trunk FM, WC and more number of MetS components also had higher 8-epi levels suggest the close relationship between oxidative stress and MetS. Our findings not only confirm the previous studies that oxidative stress is correlated with indirect body fat mass measures

(BMI and WC), but also provide evidence that regional fat mass accumulations are closely correlated with oxidative stress. Among them, lower-body FM is strongly associated with systemic oxidative stress. In addition, relationships among oxidative stress to inflammatory markers (hsCRP, PAI-1) and adipokines (leptin) were also observe in this healthy female cohort.

To our knowledge, the present study is the first to evaluate the relation between DXA regional adiposity and systemic oxidative stress indicated by urinary 8-epi-$PGF_{2\alpha}$ excretion. We found that indirect anthropometric measures of BMI and WC exhibited strong correlations with oxidative stress. However the value of these simple anthropometric measures in explaining the oxidative stress level was somewhat lower after adjustment for DXA-indices. Thus, although BMI and WC represent an useful markers of oxidative stress, DXA-indices exhibited a better independent power in predicting systemic oxidative stress. The results show that both central and peripheral fat deposits are strongly associated with oxidative stress. And more interestingly, lower-body FM has the strongest relationship with 8-epi-$PGF_{2\alpha}$. Only a few studies evaluated relationship between regional FM and oxidative stress, for example, significant correlation between serum 8-epi-$PGF_{2\alpha}$ level and abdominal visceral fat area (VFA) measured with CT was reported in 31 Japanese men by Urakawa et al. [12]. And Fujita *et al.* [16] reported that in 105 Japanese adults with or without MetS, both abdominal VFA and subcutaneous fat area (SFA) showed significant association with urinary 8-epi-$PGF_{2\alpha}$ excretion, moreover, in multiple regression analysis VFA was the strongest determinant of urinary 8-epi-$PGF_{2\alpha}$ in individuals with MetS. However, these two and other studies only emphasized FM depositing in the abdominal cavity without giving consideration to the effects of total body FM as well as other regional adiposity. Based on CT or magnetic resonance imaging (MRI), it has been estimated that in women the vast majority of FM situated subcutaneously and only 7-8% of the total body FM depots in abdominal cavity [36-38]. Therefore we believe it is more reasonable to take total and regional FM into account when concern with the relation of adiposity to systemic oxidative stress. In the current study, we found total, trunk and lower-body FM showed strong correlations with oxidative stress, even after controlling for BMI and WC. In multiple regression analysis after further taking various confounders into account, lower-body FM and PAI-1 exhibited strong power to predict systemic oxidative stress. Since in women lower-body region is a major compartment for subcutaneous FM accumulation [39, 40], it might be speculated that subcutaneous FM is an important correlate of systemic stress in healthy middle-aged women. The result is somewhat different from Urakawa's [12] and Fujita's [16] findings which suggested abdominal VFA is strongly associated with systemic oxidative stress. This maybe due to we investigate the relationship between adiposity and oxidative stress with a different view of point. General body FM distribution measured with DXA is emphasized in the present study whereas other studies concentrate on the effects of VFA and SAF located in the abdominal cavity estimated with single slice CT scan. Moreover, the subjects we studied are basically lean female adults with mean BMI, WC, FM% as 22.0kg/$m^2$, 78.9cm and 30.1%, respectively and no one could be classified as having MetS, which are quite different from Urakawa's study (male adults with mean BMI 26.9kg/$m^2$ and WC 156.9cm in obese group) and Fujita's study (male and female adults with mean BMI 28.7kg/$m^2$ and WC 96.9cm in MetS group). Unfortunately we are not able to test the association between lower-body FM and oxidative stress after correction for visceral FM because DXA cannot distinguish trunk visceral FM from subcutaneous FM. However, after adjustment for WC, a surrogate index for abdominal visceral FM [41], lower-body FM still associated with oxidative stress in our study.

The underlying mechanism(s) why subcutaneous FM represents a potent link with oxidative stress in healthy female adults is not elucidated yet. Intrinsic different metabolic activity between visceral adipocyte and subcutaneous adipocyte [42], as well as the characteristic of FM distribution of women, may provide explanations. Lipids accumulation is favored in the lower-body region of premenopausal women in comparison with men [43]. This may due to the lipoprotein lipase (LPL) activity, a key factor responsible for the liberation of the lipolytic products to the adipocyte for deposit as TG, is higher in subcutaneous fat cells than visceral adipocyte in women, but not in men [18]. On the other hand, lower-body fat cell exhibits a lower lipolytic response to catecholamine and a higher response to insulin-mediated lipogenesis than visceral adipocyte does, and showing both reduced β1- and β2-adrenoreceptor density and sensitivity and increased α2-adrenoreceptor affinity and number [18, 44, 45]. As

a result, lower-body fat cells in women are resistant to lipolysis and prone to lipogenesis. LPL is demonstrated to be able to enhance both enzymatic and non-enzymatic oxidation of LDL lipids induced by 15-lipoxygenase [46] then elevated LPL activity of lower-body FM may contribute to the activation of lipid peroxidation. Furthermore, animal experiment indicated that during the course of the repeated cycles of fasting-feeding, the changes of lipid peroxidation and lipolysis were antiparallel to each other. That means during the cycles, there was a net increase in lipid peroxidation accompanying with a net decrease in lipolysis [47, 48]. Therefore it is reasonable to assume that the reduced lipolysis in lower-body subcutaneous adipose tissue might result in a heightened lipid peroxidation. Further experiments comparing the lipid peroxidation between visceral and subcutaneous adipose tissue are needed to clarify this issue.

In this study, multiple regression analyses demonstrated that PAI-1 is another important predictor of systemic oxidative stress level. This finding consists with the observation that increased oxidative stress in cultured adipocyte is able to enhance PAI-1 mRNA expression [9] and activates PAI-1 promoter transcription [49]. Elevated PAI-1 levels is proved to be an independent risk for cardiovascular events [50, 51]. Combined with the results from the present study that urinary 8-epi-$PGF_{2\alpha}$ excretion are positively associated with hsCRP and leptin, the findings support that oxidative-stress-induced dysregulation of adipokines and inflammatory markers have already existed even in healthy women without obvious CVD risks.

Potential limitations of our study should be pointed out. Firstly, because of the cross-sectional nature of the present study we are not able to provide a causative conclusion. Second, the subjects we studied were relatively homogenous with lower CVD risks. Although various confounding factors such as sex, age, cigarette smoking and alcohol drinking have been minimized, we should be cautious to apply the conclusion to general population. Thus further extending the study samples to men and other ethnic populations with various CVD risks is needed. Moreover, lower-body FM has been demonstrated to have beneficial effects on glucose [25, 42] and lipid metabolism [17], however our findings suggest that this beneficial metabolic effects of lower-body FM might be mediated by other factors or pathways more than oxidative stress at least in healthy women.

In summary, novel findings of the present study indicate DXA-derived fat mass measures are more potent correlates with systemic oxidative stress than indirect anthropometric indices in healthy middle-aged women. Lower-body FM exhibited strong ability to predict urinary 8-epi-$PGF_{2\alpha}$ excretion, suggesting subcutaneous FM plays an important role in systemic oxidative stress. These results suggest that regional adiposity in the lower-body part should be taken into account as obesity-related phenotypes in evaluating obesity-induced systemic oxidative stress. The interrelationships among urinary 8-epi-$PGF_{2\alpha}$ excretion, PAI-1, hsCRP and leptin, combined with results of other *in vitro* studies, suggest that oxidative-stress-induced dysregulation of adipokines and inflammation might mediate adverse metabolic effects of regional adiposity.

## Acknowledgement

This study was supported by Open Research Center Project for Private University: Matching Fund Subsidy for Private Universities, The Ministries of Education, Culture, Sports, Science and Technology, Japan. We are indebted to all the participants for their dedicated and conscientious collaboration.

## References

1. Despres JP, Lemieux I (2006) Abdominal obesity and metabolic syndrome. *Nature* 444:881-887.
2. Ford ES (2005) Risks for all-cause mortality, cardiovascular disease, and diabetes associated with the metabolic syndrome: a summary of the evidence. *Diabetes Care* 28:1769-1778.
3. Hotamisligil GS, Shargill NS, Spiegelman BM (1993) Adipose expression of tumor necrosis factor-alpha: direct role in obesity-linked insulin resistance. *Science* 259:87-91.
4. Shimomura I, Funahashi T, Takahashi M, Maeda K, Kotani K, Nakamura T, Yamashita S, Miura M, Fukuda Y, Takemura K, Tokunaga K, Matsuzawa Y (1996) Enhanced expression of PAI-1 in visceral fat: possi-

ble contributor to vascular disease in obesity. *Nat Med* 2:800-803.
5. Emdin M, Pompella A, Paolicchi A (2005) Gamma-glutamyltransferase, atherosclerosis, and cardiovascular disease: triggering oxidative stress within the plaque. *Circulation* 112:2078-2080.
6. Itoh S, Umemoto S, Hiromoto M, Toma Y, Tomochika Y, Aoyagi S, Tanaka M, Fujii T, Matsuzaki M (2002) Importance of NAD (P) H oxidase-mediated oxidative stress and contractile type smooth muscle myosin heavy chain SM2 at the early stage of atherosclerosis. *Circulation* 105:2288-2295.
7. Perticone F, Ceravolo R, Candigliota M, Ventura G, Iacopino S, Sinopoli F, Mattioli PL (2001) Obesity and body fat distribution induce endothelial dysfunction by oxidative stress: protective effect of vitamin C. *Diabetes* 50:159-165.
8. Robertson RP (2004) Chronic oxidative stress as a central mechanism for glucose toxicity in pancreatic islet beta cells in diabetes. *J Biol Chem* 279:42351-42354.
9. Furukawa S, Fujita T, Shimabukuro M, Iwaki M, Yamada Y, Nakajima Y, Nakayama O, Makishima M, Matsuda M, Shimomura I (2004) Increased oxidative stress in obesity and its impact on metabolic syndrome. *J Clin Invest* 114:1752-1761.
10. Keaney JF, Jr., Larson MG, Vasan RS, Wilson PW, Lipinska I, Corey D, Massaro JM, Sutherland P, Vita JA, Benjamin EJ (2003) Obesity and systemic oxidative stress: clinical correlates of oxidative stress in the Framingham Study. *Arterioscler Thromb Vasc Biol* 23:434-439.
11. Ferroni P, Guagnano MT, Manigrasso MR, Ciabattoni G, Davi G (2005) Increased plasminogen activator inhibitor-1 levels in android obesity: correlation with oxidative stress. *J Thromb Haemost* 3:1086-1087.
12. Urakawa H, Katsuki A, Sumida Y, Gabazza EC, Murashima S, Morioka K, Maruyama N, Kitagawa N, Tanaka T, Hori Y, Nakatani K, Yano Y, Adachi Y (2003) Oxidative stress is associated with adiposity and insulin resistance in men. *J Clin Endocrinol Metab* 88:4673-4676.
13. Nakanishi S, Yamane K, Kamei N, Nojima H, Okubo M, Kohno N (2005) A protective effect of adiponectin against oxidative stress in Japanese Americans: the association between adiponectin or leptin and urinary isoprostane. *Metabolism* 54:194-199.
14. Shin MJ, Lee JH, Jang Y, Park E, Oh J, Chung JH, Chung N (2006) Insulin resistance, adipokines, and oxidative stress in nondiabetic, hypercholesterolemic patients: leptin as an 8-epi-prostaglandin F2alpha determinant. *Metabolism* 55:918-922.
15. Davi G, Guagnano MT, Ciabattoni G, Basili S, Falco A, Marinopiccoli M, Nutini M, Sensi S, Patrono C (2002) Platelet activation in obese women: role of inflammation and oxidant stress. *JAMA* 288:2008-2014.
16. Fujita K, Nishizawa H, Funahashi T, Shimomura I, Shimabukuro M (2006) Systemic oxidative stress is associated with visceral fat accumulation and the metabolic syndrome. *Circ J* 70:1437-1442.
17. Rebuffe-Scrive M, Lonnroth P, Marin P, Wesslau C, Bjorntorp P, Smith U (1987) Regional adipose tissue metabolism in men and postmenopausal women. *Int J Obes* 11:347-355.
18. Bouchard C, Despres JP, Mauriege P (1993) Genetic and nongenetic determinants of regional fat distribution. *Endocr Rev* 14:72-93.
19. Hamdy O, Porramatikul S, Al-Ozairi E (2006) Metabolic obesity: the paradox between visceral and subcutaneous fat. *Curr Diabetes Rev* 2:367-373.
20. Williams MJ, Hunter GR, Kekes-Szabo T, Snyder S, Treuth MS (1997) Regional fat distribution in women and risk of cardiovascular disease. *Am J Clin Nutr* 65:855-860.
21. Hunter GR, Kekes-Szabo T, Snyder SW, Nicholson C, Nyikos I, Berland L (1997) Fat distribution, physical activity, and cardiovascular risk factors. *Med Sci Sports Exerc* 29:362-369.
22. Van Pelt RE, Evans EM, Schechtman KB, Ehsani AA, Kohrt WM (2002) Contributions of total and regional fat mass to risk for cardiovascular disease in older women. *Am J Physiol Endocrinol Metab* 282:E1023-1028.
23. Roberts LJ, 2nd, Morrow JD (1997) The generation and actions of isoprostanes. *Biochim Biophys Acta* 1345:121-135.
24. Goodpaster BH (2002) Measuring body fat distribution and content in humans. *Curr Opin Clin Nutr Metab Care* 5:481-487.
25. Snijder MB, Dekker JM, Visser M, Bouter LM, Stehouwer CD, Yudkin JS, Heine RJ, Nijpels G, Seidell JC (2004) Trunk fat and leg fat have independent and opposite associations with fasting and postload glucose levels: the Hoorn study. *Diabetes Care* 27:372-377.
26. Mazess RB, Barden HS, Bisek JP, Hanson J (1990) Dual-energy x-ray absorptiometry for total-body and regional bone-mineral and soft-tissue composition. *Am J Clin Nutr* 51:1106-1112.
27. Svendsen OL, Haarbo J, Hassager C, Christiansen C (1993) Accuracy of measurements of body composition by dual-energy x-ray absorptiometry *in vivo*. *Am J Clin Nutr* 57:605-608.
28. Matthews DR, Hosker JP, Rudenski AS, Naylor BA, Treacher DF, Turner RC (1985) Homeostasis model assessment: insulin resistance and beta-cell function from fasting plasma glucose and insulin concentrations in man. *Diabetologia* 28:412-419.
29. Friedewald WT, Levy RI, Fredrickson DS (1972) Estimation of the concentration of low-density lipoprotein cholesterol in plasma, without use of the preparative ultracentrifuge. *Clin Chem* 18:499-502.

30. Hirano T, Ito Y, Saegusa H, Yoshino G (2003) A novel and simple method for quantification of small, dense LDL. *J Lipid Res* 44:2193-2201.
31. (2000) WHO Western Pacific Regional Office, IOTF, IASO, *The Asia-Pacific perspective: redefining obesity and its treatment*, In: Health Communications Australia Sydney.
32. (2001) Executive Summary of The Third Report of The National Cholesterol Education Program (NCEP) Expert Panel on Detection, Evaluation, And Treatment of High Blood Cholesterol In Adults (Adult Treatment Panel III). *JAMA* 285:2486-2497.
33. Alberti KG, Zimmet P, Shaw J (2006) Metabolic syndrome—a new world-wide definition. A Consensus Statement from the International Diabetes Federation. *Diabet Med* 23:469-480.
34. Matsuzawa Y (2005) Metabolic syndrome—definition and diagnostic criteria in Japan. *J Atheroscler Thromb* 12:301.
35. Ceriello A, Motz E (2004) Is oxidative stress the pathogenic mechanism underlying insulin resistance, diabetes, and cardiovascular disease? The common soil hypothesis revisited. *Arterioscler Thromb Vasc Biol* 24:816-823.
36. Sohlstrom A, Wahlund LO, Forsum E (1993) Adipose tissue distribution as assessed by magnetic resonance imaging and total body fat by magnetic resonance imaging, underwater weighing, and body-water dilution in healthy women. *Am J Clin Nutr* 58:830-838.
37. Ludescher B, Najib A, Baar S, Machann J, Thamer C, Schick F, Buchkremer G, Claussen CD, Eschweiler GW (2007) Gender specific correlations of adrenal gland size and body fat distribution: a whole body MRI study. *Horm Metab Res* 39:515-518.
38. Lemieux S, Prud'homme D, Bouchard C, Tremblay A, Despres JP (1993) Sex differences in the relation of visceral adipose tissue accumulation to total body fatness. *Am J Clin Nutr* 58:463-467.
39. Goodpaster BH, Thaete FL, Simoneau JA, Kelley DE (1997) Subcutaneous abdominal fat and thigh muscle composition predict insulin sensitivity independently of visceral fat. *Diabetes* 46:1579-1585.
40. Goodpaster BH, Thaete FL, Kelley DE (2000) Thigh adipose tissue distribution is associated with insulin resistance in obesity and in type 2 diabetes mellitus. *Am J Clin Nutr* 71:885-892.
41. Pouliot MC, Despres JP, Lemieux S, Moorjani S, Bouchard C, Tremblay A, Nadeau A, Lupien PJ (1994) Waist circumference and abdominal sagittal diameter: best simple anthropometric indexes of abdominal visceral adipose tissue accumulation and related cardiovascular risk in men and women. *Am J Cardiol* 73:460-468.
42. Tran TT, Yamamoto Y, Gesta S, Kahn CR (2008) Beneficial effects of subcutaneous fat transplantation on metabolism. *Cell Metab* 7:410-420.
43. Arner P, Lithell H, Wahrenberg H, Bronnegard M (1991) Expression of lipoprotein lipase in different human subcutaneous adipose tissue regions. *J Lipid Res* 32:423-429.
44. Mauriege P, Marette A, Atgie C, Bouchard C, Theriault G, Bukowiecki LK, Marceau P, Biron S, Nadeau A, Despres JP (1995) Regional variation in adipose tissue metabolism of severely obese premenopausal women. *J Lipid Res* 36:672-684.
45. Reynisdottir S, Wahrenberg H, Carlstrom K, Rossner S, Arner P (1994) Catecholamine resistance in fat cells of women with upper-body obesity due to decreased expression of beta 2-adrenoceptors. *Diabetologia* 37:428-435.
46. Neuzil J, Upston JM, Witting PK, Scott KF, Stocker R (1998) Secretory phospholipase A2 and lipoprotein lipase enhance 15-lipoxygenase-induced enzymic and nonenzymic lipid peroxidation in low-density lipoproteins. *Biochemistry* 37:9203-9210.
47. Rejholcova M, Wilhelm J (1989) Lipid peroxidation and lipolysis during fasting. *Acta Univ Carol [Med]* (Praha) 35:43-61.
48. Rejholcova M, Wilhelm J, Svoboda P (1988) Lipid peroxidation inhibits norepinephrine- stimulated lipolysis in rat adipocytes. Reduction of beta-adreno-ceptor number. *Biochem Biophys Res Commun* 150:802-810.
49. Vulin AI, Stanley FM (2004) Oxidative stress activates the plasminogen activator inhibitor type 1 (PAI-1) promoter through an AP-1 response element and cooperates with insulin for additive effects on PAI-1 transcription. *J Biol Chem* 279:25172-25178.
50. Landin K, Tengborn L, Smith U (1990) Elevated fibrinogen and plasminogen activator inhibitor (PAI-1) in hypertension are related to metabolic risk factors for cardiovascular disease. *J Intern Med* 227:273-278.
51. Juhan-Vague I, Alessi MC (1997) PAI-1, obesity, insulin resistance and risk of cardiovascular events. *Thromb Haemost* 78:656-660.

**Laboratory Investigation (2009) 89, 1340–1347**


# Timp-3 deficiency impairs cognitive function in mice

Yoshichika Baba[1], Osamu Yasuda[1], Yukihiro Takemura[1], Yasuyuki Ishikawa[2], Mitsuru Ohishi[1], Jun Iwanami[3], Masaki Mogi[3], Nobutaka Doe[4], Masatsugu Horiuchi[3], Nobuyo Maeda[5], Keisuke Fukuo[6] and Hiromi Rakugi[1]

Extracellular matrix (ECM) degradation is performed primarily by matrix metalloproteinases (MMPs). MMPs have recently been shown to regulate synaptic activity in the hippocampus and to affect memory and learning. The tissue inhibitor of metalloproteinase (Timp) is an endogenous factor that controls MMP activity by binding to the catalytic site of MMPs. At present, four Timp isotypes have been reported (Timp-1 through Timp-4) with 35–50% amino-acid sequence homology. Timp-3 is a unique member of Timp proteins in that it is bound to the ECM. In this study, we used the passive avoidance test, active avoidance test, and water maze test to examine the cognitive function in Timp-3 knockout (KO) mice. Habituation was evaluated using the open-field test. The water maze test showed that Timp-3 KO mice exhibit deterioration in cognitive function compared with wild-type (WT) mice. The open-field test showed decreased habituation of Timp-3 KO mice. Immunostaining of brain slices revealed the expression of Timp-3 in the hippocampus. *In situ* zymography of the hippocampus showed increased gelatinolytic activity in Timp-3 KO mice compared with WT mice. These results present the first evidence of Timp-3 involvement in cognitive function and hippocampal MMP activity in mice. Moreover, our findings suggest a novel therapeutic target to be explored for improvement of cognitive function in humans.

*Laboratory Investigation* (2009) **89,** 1340–1347; doi:10.1038/labinvest.2009.101; published online 5 October 2009

**KEYWORDS:** cognitive function; extracellular matrix; hippocampus; matrix metalloproteinase; Timp-3

Extracellular matrix (ECM) molecules have important roles in the structural changes of brain synapses involved in neural plasticity, learning, and memory.[1] ECM interacts with cells through cell surface receptors, such as integrin, cadherin, and neural adhesion molecules,[2] and these interactions affect cell proliferation, growth, migration, synaptic stabilization, and apoptosis. Thus, the ECM develops a wide range of signals within the brain tissue.[3]

Matrix metalloproteinases (MMPs) comprise a family of protein-digesting enzymes that have an important role in structural maintenance and conversion of the ECM.[4] MMPs target many substrates, including proteases, growth factors, cytokines, cell surface receptors, and cell adhesion molecules.[5] Excess activation of MMPs occurs under several pathophysiological conditions, such as rheumatoid arthritis and rupture of atherosclerotic plaques.[6–8] Thus, MMP activity is tightly controlled at the level of transcription, activation of the precursor zymogens, and inhibition by the tissue inhibitors of metalloproteinase (Timp).[9]

At present, four members of the Timp family (Timp-1 to Timp-4), possessing 35–50% amino-acid sequence homology, have been identified. All Timp isotypes contain 12 cysteines that form 6 disulfide bonds. To inhibit MMP activity, Timp proteins form a 1:1 complex with a zinc-binding site in the catalytic region of MMP.[10]

Each Timp protein has unique characteristics. Timp-1, Timp-2, and Timp-4 are present in soluble form.[11–13] Timp-3, which is tightly bound to the ECM, is involved in cell proliferation, apoptosis, and angiogenesis.[11–13] Timp-1 binds to proMMP-9, Timp-2 binds to proMMP-2, and Timp-3 binds to both proMMP-2 and proMMP-9.[13,14]

In the central nervous system, the MMP/Timp system is responsive to changes in neural activity.[15] Deregulation of MMP activity is involved in various neurological diseases,

[1]Department of Geriatric Medicine, Osaka University Graduate School of Medicine, Suita, Osaka, Japan; [2]Division of Structural Cell Biology, Nara Institute of Science and Technology, Takayama-cho, Ikoma, Nara, Japan; [3]Department of Molecular Cardiovascular Biology and Pharmacology, Ehime University, Graduate School of Medicine, Shitsukawa, Tohon, Ehime, Japan; [4]Section of Behavioral Science, Kouiken Co. Ltd., Akashi, Hyogo, Japan; [5]Department of Pathology and Laboratory Medicine, School of Medicine, The University of North Carolina at Chapel Hill, Chapel Hill, NC, USA and [6]Department of Food Sciences and Nutrition, School of Human Environmental Sciences, Mukogawa Woman's University, Nishinomiya, Hyogo, Japan

Correspondence: Dr O Yasuda, MD, PhD, Department of Geriatric Medicine, Osaka University Graduate School of Medicine, 2-2 Yamadaoka, Suita, Osaka 565-0871, Japan.

E-mail: yasuda@geriat.med.osaka-u.ac.jp

Received 16 February 2009; revised 27 July 2009; accepted 20 August 2009

including multiple sclerosis, infection with human immunodeficiency virus, and spinal cord injury.[16–18] Moreover, MMPs are implicated in the invasion of malignant glioma cells into the brain parenchyma.[19]

In Alzheimer's disease, MMP inhibits angiogenesis and accumulation of amyloid-$\beta$.[16,20,21] Recently, MMPs have been reported to control synaptic activity in the hippocampus and to affect learning and memory.[22] Other studies have clarified the contributions of Timp-1 and Timp-2 in learning and memory. Mice deficient for Timp-1 or Timp-2 exhibit defective memory function.[23–25] Conversely, mice overexpressing Timp-1 showed a slight, but significant, improvement in learning and memory.[24] However, there is no published evidence for a role of Timp-3 in the regulation of cognitive function.

This study investigated the effects of Timp-3 on learning and memory. We conducted various behavioral tests with wild-type (WT) and Timp-3 knockout (KO) mice, and further examined the expression of Timp-3 and compared gelatinolytic activity in WT and KO brain tissues.

## MATERIALS AND METHODS

### Timp-3 KO Mice

Timp-3 KO mice were produced using the gene-targeting technique described by Kawamoto *et al*.[26] Briefly, mice carrying the mutant allele were backcrossed with C57BL/6 mice to generate KO mice in a C57BL/6 background. Genotyping of mice was performed by PCR using tail DNA.[26]

### Experimental Conditions for Behavioral Tests

All behavioral tests were conducted in the laboratory at 22 °C and 55% (50–60%) humidity. Illumination for the experimental device was set at 250 lx. The ventilation fan provided a masking noise of 40 dB, which was deemed appropriate for behavioral tests.

Mice were maintained in individual acrylic cages and naturalized to the environment during the 3 days before testing. They were given access to dry, solid feed (Labo MR Stock from Nihon Nosan, Yokohama, Japan) *ad libitum*. The room was maintained on a 12-h light and dark cycle, with the light cycle starting at 0800 hours and ending at 2000 hours. All tests were started after 1000 hours and conducted during the light period.

The passive avoidance test and water maze test with an invisible platform were conducted with 12 male WT mice and 12 KO mice. The open-field habituation test, active avoidance test, and water maze test with a visible platform were conducted using a different set of 12 male WT mice and 12 KO mice.

The experimental protocols were approved by the Osaka University Medical School Animal Care and Use Committee, and performed according to the Osaka University Medical School Guidelines for the Care and Use of Laboratory Animals.

### Passive Avoidance Test

An avoidance-learning box was constructed, with a lighted chamber ($15 \times 15 \times 20\,cm^3$) and dark chamber ($15 \times 15 \times 20\,cm^3$) connected to each other. A guillotine door separated the two compartments. A mouse was placed in the lighted chamber, and the guillotine door was opened. When the mouse spontaneously moved into the dark chamber, the guillotine door was closed. Within 10 s, a 3-s, 160-V AC electrical shock was delivered through the grid floor. The latency period for the mouse to enter the dark chamber was recorded. After this single learning trial, the mouse was immediately removed from the device.

After 24 h, the same mouse was put in the lighted chamber for the single retention test. The latency period ($\leq 300$ s) for the mouse to enter the dark chamber was recorded. No electric shock was given during the retention test.

### Active Avoidance Test

An avoidance-learning box with two connecting compartments (each $15 \times 15 \times 20\,cm^3$) was constructed. The mouse was able to move freely between the two compartments. To detect movement, two infrared ray beams were attached on both walls on the sides of each compartment, 2 cm above the floor and 5 cm from the gate. The avoidance-learning box, which was placed in a ventilated, sound-attenuating chamber to maintain a background noise level of 64 dB throughout the session, was indirectly illuminated by white bulbs fixed to the ceiling of the chamber. A 1500-Hz pure tone with 85 dB of sound pressure was used as a conditioned stimulus (CS), and a 140-V AC electrical shock delivered from the grid floor was used as an unconditioned stimulus (US).

A mouse was placed in one compartment and allowed to move between the two compartments throughout the training session. The US, which was delivered from the grid floor 5 s after the CS was delivered, overlapped for a maximum of 15 s. When the mouse moved to the connecting compartment within 5 s from the time of the CS, the US was not delivered, and the movement of the mouse was counted as avoidance behavior. When the mouse failed to move to the connecting compartment, the US was delivered. Both the CS and US were terminated immediately when the mouse moved to the connecting compartment after the onset of the US. The number of migration reactions in inter-trial intervals (25 s on average) was measured as an indicator of spontaneous activity. This active avoidance test was performed for 3 consecutive days, with one 50-trial session per day.

### Water Maze Test

The water maze test was conducted using a round pool (inside diameter = 95 cm; depth = 35 cm) filled with water, made opaque by the addition of titanium oxide to a depth of 22 cm. The temperature of the water was maintained at $22 \pm 1$ °C using a thermostatic heater. The pool was set on a pedestal (30 cm in height), and was enclosed (area = $130 \times 130\,cm^2$) by four white walls (120 cm in

height). As extra-maze cues, letter-sized posters, a CCD camera, and a black doll (20 cm in height) were attached to the walls.

In the invisible platform test, a clear, round platform (diameter = 10 cm) was submerged 0.5 cm below the surface of the water. Training trials were conducted for 5 consecutive days, with 5 trial sessions per day. In the three quadrants away from the platform, a mouse placed near the wall was released into the pool. The releasing quadrants varied with pseudo-random sequences for each mouse. The escape latency period (measured for a maximum of 60 s) was defined as the time it took for a mouse to reach the platform. The training trial terminated when the mouse reached the platform and remained on it for 10 s. In cases in which the mouse did not find the platform within 60 s, the mouse was guided to the platform by the experimenter and was kept on the platform for 10 s. On the day after 5 consecutive days of access training, the platform was removed, and a 1-min probe test was performed. The 1-min probe test measured latency time in the quadrant in which the platform was previously placed.

The visible platform test was conducted independently using a different group of 12 WT and 12 KO mice (ie, different groups of mice from those used in the invisible platform test). Methodology for the visible platform test was similar, except (1) the platform was not submerged, but rather was placed 0.5 cm above the surface of the water, and (2) as a cue, a stick with a black cube on top was placed on the platform.

### Open-Field Habituation Test

The apparatus for the open-field habituation test was manufactured by Taiyo Electric. (Tokyo, Japan). WT and KO mice were placed in an acrylic box ($30 \times 30 \times 30\,cm^3$) stored within a ventilated, soundproof chamber. An incandescent bulb, which was fixed to the ceiling of the chamber, provided lighting of ~110 lx in the chamber. A fan attached to the wall of the chamber produced a masking noise of 45 dB. Habituation of the mice to the environment was measured as a function of locomotion and rearing behavior. The number of episodes of locomotion and rearing behavior, which were recorded with infrared ray beams placed on the lateral side of the box, was scored. The open-field habituation test was conducted for 3 days, with one 10-min session per day.

### Reverse Transcription-PCR

RNA was isolated from mouse hippocampus using the ISOGEN (Nippon Gene, Tokyo, Japan) kit, according to the manufacturer's instructions. *Timp-3* gene expression was detected by reverse transcribing the isolated RNA and amplifying the product with PCR (RT-PCR). The PCR amplification was performed with the following primers: Timp-3: Timp-3F, 5′-CACGGAAGCCTCTGAAAGTC-3′, and Timp-3R, 5′-CCCAAAATTGGAGAGCATGT-3′. GAPDH: GAPDH-F, 5′-AAATGGTGAAGGTCGGTGTG-3′, and GAPDH-R, 5′-GCAGAAGGGGCGGAGATGAT-3′.

### Immunostaining

WT and Timp-3 KO mice were killed, and their brains were collected, fixed with formaldehyde, embedded in paraffin, and cut into 10-$\mu$m-thick sections with a microtome. To remove endogenous peroxidase, the sections were treated with 0.3% hydrogen peroxide in methanol at room temperature. The sections were washed with 0.05 M phosphate buffer (pH 7.6) thrice for 3 min. The sections were then treated with phosphate buffer containing 0.5% bovine serum albumin and 0.1% sodium azide for 10 min at room temperature. This was performed to absorb nonspecific proteins. Subsequently, the sections were allowed to react with the anti-Timp-3 rabbit polyclonal antibody (ProteinTech, Chicago, IL, USA) (500 × dilution) overnight at 4 °C. Next, the sections were washed thrice for 3 min with 0.05 M phosphate buffer (pH 7.6), and then allowed to react for 30 min with the secondary antibody conjugated with peroxidase. Thereafter, the sections were again washed with 0.05 M phosphate buffer. After a 5-min chromogenic reaction with 3,3′-Diaminobenzidine HCl, the sections were counterstained with Mayer's hematoxylin for 5 min. The sections were then dehydrated and encapsulated for observation under an optical microscope.

### *In Situ* Zymography

Gelatinolytic activity in mouse brain sections was determined by *in situ* zymography with DQ-gelatin-FITC (Molecular Probes, Eugene, OR, USA) as described previously.[27,28] Briefly, unfixed whole mouse brain was embedded in OCT compound. Sections (of 10-$\mu$m thickness) were cut and air dried for 1 h, re-hydrated in PBS, and incubated at 37 °C in DQ-gelatin-FITC solution (100 $\mu$g/ml in PBS) for 1 h. Sections were then washed thrice in PBS, fixed in 4% paraformaldehyde, and examined under a fluorescent microscope to detect green fluorescence due to gelatinolytic activity.

### Statistical Analysis

Results are expressed as mean ± s.e. Comparison among groups was performed by one-way ANOVA; Student's *t*-test was used when appropriate. A value of $P<0.05$ was considered significant.

## RESULTS

### Passive Avoidance Test

WT and KO mice first underwent preconditioning. When a mouse moved from the lighted chamber into the dark chamber, it received an electric shock. Twenty-four hours after preconditioning, one retention trial was performed. In the retention trial, the latency time in the lighted chamber was measured and compared between the two mice groups. As a result of receiving an electric shock in the dark chamber, the mean latency time in the retention trial was prolonged in

both WT and KO mice, indicating that both types of mice acquired avoidance memory. Moreover, no significant difference was observed in latency times for WT and KO mice, either before ($54.4 \pm 19.5$ s for WT, $27.7 \pm 7.5$ s for KO; $P = 0.20$) or after ($300 \pm 0.0$ s for WT, $276 \pm 18.7$ s for KO; $P = 0.23$) conditioning. These results show that there were no memory deficits in KO mice compared with WT mice.

### Active Avoidance Test

WT and KO mice were placed in the avoidance-learning box with two compartments connected. A beep was presented, and 5 s later, an electronic shock was given through the grid floor. When this process was repeated, the mice learned to escape the shock by migrating into the adjoining compartments at the sound of the beep. A migration reaction within 5 s from the beep was defined as the 'avoidance' reaction. The number of avoidance reactions was counted over 3 days, with 50 trials per day. Moreover, the number of migrations between trial intervals in the absence of stimuli was counted to compare general activity levels.

We found no differences in activity levels between WT and KO mice over the 3 days of testing ($F(1,22) = 1.88$, $P = 0.183$). Successful avoidance increased in both WT and KO mice as a function of training days, indicating that both types of mice acquired avoidance memory. Furthermore, there was no difference between the number of avoidance reactions in WT and KO mice during the 3 days of testing ($F(1,22) = 0.46$, $P = 0.505$). These results indicate that no memory deficits were detected in KO mice.

### Water Maze Test with Invisible Platform

The water maze test with the invisible platform was conducted to evaluate spatial memory in WT and KO mice. Each mouse underwent 5 access tests daily for 5 consecutive days. Escape latency period was defined as the time (measured for a maximum of 60 s) it took for each mouse to reach the platform submerged in the pool of opaque water.

On the first day, no significant difference was observed between WT and KO mice. However, on the second day, memory acquisition in KO mice was significantly reduced compared with WT mice. Although a significant difference in memory acquisition was also observed on the third and fourth days, the difference gradually decreased (Figure 1a), and the difference in memory acquisition was no longer significant on day 5.

To measure the time spent in the quadrant in which the platform had been previously placed, a 1-min probe test was conducted the day after (ie, on day 6) completion of the access tests. The time spent in the target quadrant was longer than that achieved merely by chance, indicating that both types of mice acquired memory of the previous location of the platform. Moreover, no significant difference was observed in the time that WT or KO mice spent in the target quadrant ($19.6 \pm 1.71$ s for WT; $20.9 \pm 1.27$ s for KO; $P = 0.561$).

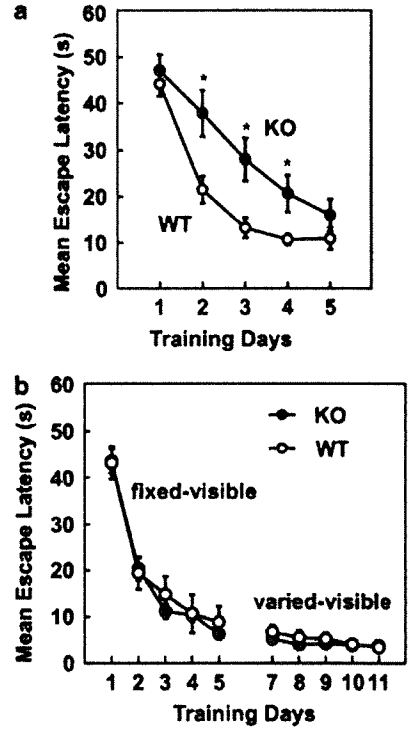


**Figure 1** Water maze tests. (**a**) Invisible platform test of wild-type (WT; $n = 12$) and Timp-3 knockout (KO; $n = 12$) mice. A clear, round platform was submerged 0.5 cm beneath the surface of milk-colored water in a pool. Escape latency period is the time (measured for a maximum of 60 s) it took for each mouse entering the pool to reach the submerged, invisible platform. Training trials were performed for 5 consecutive days, with 5 trial sessions per day. Data are expressed as mean ± s.e. $^*P < 0.05$. (**b**) Visible platform test of WT ($n = 12$) and Timp-3 KO ($n = 12$) mice. The platform was placed 0.5 cm above the surface of water in a pool. As a visual cue, a stick with a black cube on top was placed on the platform. The location of the platform was fixed from day 1 through day 5, and varied from day 7 through day 11. Escape latency period (measured for a maximum of 60 s) is the time it took for each mouse, after entering the pool, to reach the visible platform. Five trial sessions were performed per day. Data are expressed as mean ± s.e.

Taken together, these results indicate that although KO mice eventually learned the location of the platform, their speed in acquiring memory was significantly slower than that of WT mice.

### Water Maze Test with Visible Platform

In humans, a Timp-3 mutation causes Sorsby's fundus dystrophy (SFD), a disease characterized by the loss of central vision during the fourth or fifth decade of life. It is likely that the KO mice used in this study were able to recognize visual cues, given that they eventually learned the location of the platform. This conclusion is supported by a previous study showing that learning in water maze tests relies on the use of visual cues.[29] To further investigate whether KO mice were able to use visual cues during a water maze test, a visible platform test was conducted.

The mean escape latency period gradually decreased from day 1 to day 5 in both WT and KO mice, indicating that both types of mice acquired memory of the location of the platform (Figure 1b). Mean escape latency times for WT and KO mice were similar during the 5 days of testing. This finding indicates that both types of mice approached the platform aided by the visible cue, rather than by spatial memory. Moreover, the results suggest that the swimming ability of KO mice was not compromised. Moreover, latency times of WT and KO mice were not different, even when the location of the visible platform was varied (on days 7 through 11). The fact that latency time at day 7, the first day in the varied visible platform test, was not longer than that at day 5, the last day in the fixed visible platform test, also indicates that both types of mice approached the platform aided by the visual cue rather than by spatial memory.

Probe tests conducted on day 6 ($13.0 \pm 1.40$ s for WT; $15.4 \pm 0.97$ s for KO; $P = 0.162$) and day 12 ($12.5 \pm 1.18$ s for WT; $12.9 \pm 0.98$ s for KO; $P = 0.821$) also showed no difference in latency times between WT and KO mice. Furthermore, latency times observed for both types of mice were not longer than the latency times expected if achieved merely by chance. These results also indicate that movement of mice in the visible platform test was dependent on the use of visual cues, rather than on memory of the location of the platform.

Taken together, our findings suggest that KO mice were able to recognize visual cues in the water maze test. An alternative interpretation is that visual failure in KO mice was minimal and did not substantially compromise the recognition of visual cues.

## Open-Field Habituation Test

To evaluate the motion and mobility of the mice, the numbers of locomotion and rearing were scored for 10 min per day for 3 days with sensors placed on the lateral side of the chamber. There was no significant difference between WT and KO mice in the numbers of locomotion ($107.8 \pm 5.76$ in WT, $116.9 \pm 10.76$ in KO; $P = 0.490$) and rearing ($99.2 \pm 6.95$ in WT, $91.6 \pm 9.19$ in KO; $P = 0.535$) on day 1; however, significant differences were observed on day 3 (Figure 2a and b). Both locomotion and rearing decreased over time in WT mice, but did not substantially change over time in KO mice. This indicated that WT, but not KO, mice became accustomed to the environment.

## Timp-3 Expression in the Brain

RT-PCR showed the expression of Timp-3 in the hippocampus of WT mice (Figure 3a). In contrast, no Timp-3 was

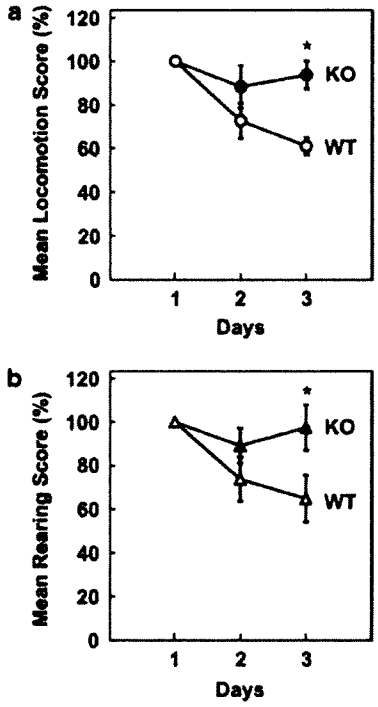


**Figure 2** Open-field habituation test. (**a**) The graph shows the change in locomotion score for WT ($n = 12$) and Timp-3 KO ($n = 12$) mice over time (days). The locomotion score, which represents the number of migrations of each mouse in a period of 10 min, is expressed as a percentage. Data are expressed as mean ± s.e. $^*P < 0.05$. (**b**) The graph shows changes in rearing score in WT ($n = 12$) and Timp-3 KO ($n = 12$) mice over time (days). The rearing score, which represents the number of times that each mouse rose (ie, exhibited rearing behavior) in a period of 10 min, is expressed as a percentage. Data are expressed as mean ± s.e. $^*P < 0.05$.

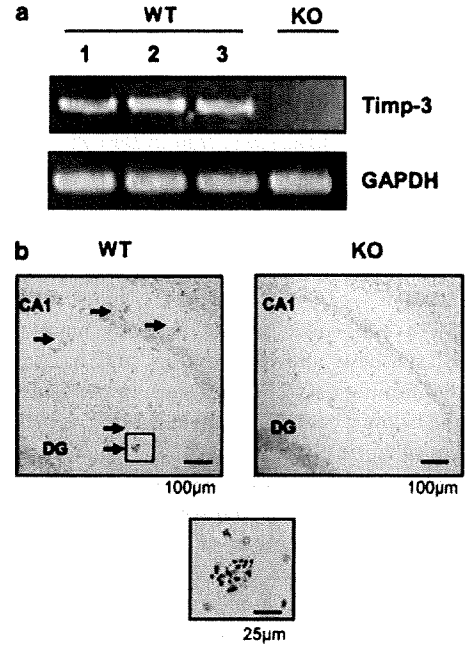


**Figure 3** Expression of Timp-3 in the hippocampus. (**a**) RT-PCR of the *Timp-3* gene. RT-PCR was performed with RNA isolated from the hippocampus of wild-type (WT) and three different Timp-3 knockout (KO) mice. Amplification of the glyceraldehyde-3-phosphate dehydrogenase gene (GAPDH) served as a control. (**b**) Immunostaining of Timp-3. A Timp-3 antibody was hybridized to mouse brain sections and visualized with 3-3′-diaminobenzidine and a hematoxylin counterstain. Timp-3 expression is indicated in the hippocampus with arrows. The boxed region shown below is magnified × 4 to illustrate Timp-3 staining. DG, dentate gyrus.

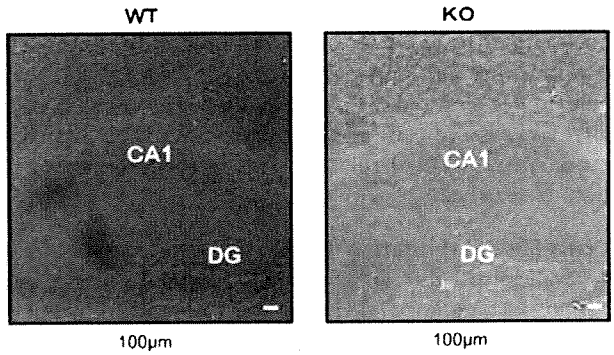


**Figure 4** *In Situ* zymography. *In situ* zymography shows the gelatinolytic activity (green fluorescence) of enzymes in the brains of wild-type (WT) and Timp-3 knockout (KO) mice. Representative photographs are shown. DG, dentate gyrus.

detected in the hippocampus of KO mice. Timp-3 expression was confirmed by immunostaining brain slices. Timp-3 was expressed in the choroid plexus (not shown) and in the hippocampus (Figure 3b). This was consistent with the results from the water maze test, because the hippocampus is considered to be directly involved in memory process.

### *In Situ* Zymography

*In situ* zymography showed that gelatinolytic activity was enhanced in the hippocampus of KO mice compared with that of WT mice. This result was reproducible in four independent experiments. Data from a representative experiment are shown in Figure 4. This result indicated that gelatinolytic enzyme activity was more active in the KO than in WT mice brains.

## DISCUSSION

The ECM in a normal, healthy tissue is maintained by a balance of synthesis and degradation, and has a significant role in maintaining tissue homeostasis. In the central nervous system, the balance between Timp and MMP is believed to be involved in synaptic plasticity, particularly in the mechanisms underlying memory. Previous reports have shown that ECM molecules activated signal transduction pathways through diverse cell surface receptors.[1] For example, integrins, the primary laminin receptors, are expressed in the adult hippocampus[30] and are involved in the stabilization of LTP.[31] In this paper, we have shown that Timp-3 KO mice showed increased MMP activity in the hippocampus and impaired cognitive function compared with WT mice. Similarly, Timp-1-deficient mice also showed learning and memory disturbances.[23,24] This result could also be explained by the fact that Timp-1 is expressed in the hippocampus, and synaptic plasticity is influenced by an increase in MMP activity. Timp-2 is also suggested to be involved in synaptic plasticity underlying learning and memory.[25]

We conducted behavioral tests and brain tissue analyses in Timp-3 KO mice to clarify the involvement of Timp-3 in cognitive function. Three behavioral tests were used to evaluate memory function, and an open-field test was used to evaluate habituation. We detected a decline in memory function in KO mice in the water maze test with the invisible platform, but not in passive or active avoidance tests.

Immunostaining showed the presence of Timp-3 in the hippocampus, which is considered to be the main brain region involved in memory. Moreover, *in situ* zymography showed that the hippocampi of Timp-3 KO mice had more gelatinolytic activity than did WT mice, indicating that MMP activity was deregulated in Timp-3 KO mice. Whether hippocampal deregulation of enzymatic activity in Timp-3 KO mice is directly or indirectly involved in delayed acquisition of memory in the water maze test remains to be elucidated. Moreover, it is not known whether other regions of the brain contribute to the abnormality observed in Timp-3 KO mice. Consistent with a previous report, Timp-3 expression was also detected in the choroid plexus.[32]

During central nervous system development, Timp-3 is expressed in the embryonic ventricular zone and postnatal subventricular zone, where neurogenesis occurs.[33] In addition, Timp-3 is expressed in the rostral migratory stream; a sub-population of cells in the subventricular zone migrates along the rostral migratory stream to the olfactory bulb, where cells differentiate into neurons. It is possible that lack of Timp-3 expression during brain development might have long-term effects on cognition, given that impaired cognitive function was observed in adult Timp-3 KO mice in this study.

In the water maze test using a visible platform, Timp-3 KO mice were able to use visual cues to reach the platform. However, in humans mutations in the Timp-3 gene result in SFD, a disease characterized by the loss of central vision during the fourth or fifth decade of life. A possible explanation for the discrepancy is that the Timp-3 KO mice we used were relatively young (3 months old). Alternatively, the difference in the nature of genetic alterations in SFD patients *versus* Timp-3 KO mice is another possibility. Most mutations observed in the *Timp-3* gene in SFD patients involve either the introduction of a new cysteine residue in the C-terminal domain or the presence of an odd number of cysteine residues because of the introduction of a stop codon.[34] Some of these SFD mutations may result in production of higher molecular-weight protein complexes, possibly dimers.[35] Dimerized Timp-3 protein has an active role in the SFD disease process by accumulating in the eyes.[35] In a study of eye tissues obtained from SFD patients, the thickened Bruch's membrane was strongly Timp-3 positive, except for sites where the retinal pigment epithelial cells, which normally produce Timp-3, had degenerated.[36] In contrast, Timp-3 KO mice do not express Timp-3 transcripts, do not synthesize Timp-3 protein, and do not accumulate Timp-3 protein in the eye tissue. On the basis of these observations,